INDUSTRIAL mathematics

1961

INDUSTRIAL MATHEMATICS

THE JOURNAL OF THE INDUSTRIAL MATHEMATICS SOCIETY

EDITED BY

RICHARD L. JUSTICE

VOLUME 11, PART 2

1961

THE INDUSTRIAL MATHEMATICS SOCIETY
DETROIT, MICHIGAN

Copyright 1960, by the Industrial Mathematics Society
100 Farnsworth Avenue, Detroit 2, Michigan
Library of Congress Catalog Card Number 53-39635

EDITORIAL STAFF

Managing Editors

R. L. Justice

Assistant Editors

R. Davies
J. Glover
L. Johnson
A. Mennone

LITHOPRINTED IN THE UNITED STATES OF AMERICA BY
CUSHING - MALLOY, INC., ANN ARBOR, MICHIGAN, 1962

FOREWORD

The Industrial Mathematics Society is a professional organization whose objective it is to extend the understanding and application of mathematics in industry. Founded early in 1949, it marked the first organized attempt of any group to foster a closer relationship between mathematics and industry.

It promotes the cause of mathematics in industry through monthly meetings at which technical papers are presented, through panel groups which concentrate in specialized fields of knowledge, and through publication of worthwhile papers in its annual volume.

Membership is open to engineers, scientists, and mathematicians who are concerned with the effective use of mathematics in industry. Annual dues are $5.00 per year including a subscription to the annual volume, *Industrial Mathematics*. Application forms and information may be obtained by writing to the Secretary, Industrial Mathematics Society, 100 Farnsworth, Detroit 2, Michigan.

EXECUTIVE OFFICERS
INDUSTRIAL MATHEMATICS SOCIETY

President, Joseph Rackle, Ford Motor Company, Engineering Staff
Vice President, Walter Kotoucek, Ford Motor Company, Engineering Staff
Treasurer, John Glover, Ford Motor Company, Transmission and Chassis Division
Secretary, William Buell, Ford Motor Company, Engineering Staff

1.

2.

3.

4.

5.

CONTENTS

		Page
1.	The Nature of the Helical Gear Oblique Contact Line. . . . . E. J. Wellauer	1
2.	Basic Geometry and Tooth Contact of Hypoid Gears . . . . . Meriwether L. Baxter, Jr.	19
3.	Stress Concentration Caused by a Small Circular Hole in a Bent Plate . . . . . Lajos Imre Nagy	43
4.	A Graph for Determining CSP-5 Continuous Sampling Plans. . . . . John S. White	51
5.	Introduction to Nonlinear Tchebycheff Approximation . . . . . John R. Rice	55

1

Th
Co

te
we

"P
fre
of
op

Ma

fac
ge
an

s

It
m
iz

af

1

The Nature of the Helical Gear Oblique Contact Line

By E. J. Wellauer
Director, Research and Development
The Falk Corporation

The oblique line-of-contact of helical gears has certain characteristics which merit attention by the practical gear designer as well as by the mathematical analyst.

The "oblique" line-of-contact of helical gears in contrast to the "Parallel-to-axis" contact of spur gears provides a third degree of freedom. An understanding of this greater versatility in the nature of the helical gear oblique contact line leads to its useful control for optimum gear performance.

This paper abstracts a lecture presented before the Industrial Mathematics Society.

As a means to improve the smoothness of spur gear action the face width is sometimes divided and the individual sections staggered to develop step gears. With continued divisions, the appearance of the helical gear tooth is approached as shown in Figure 1.

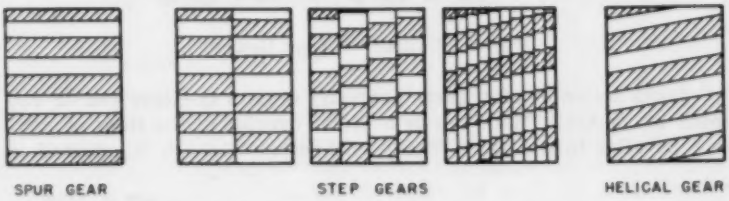

Fig. 1. Development of Helical Gear Action.

It is important to indicate that the ultimate contact does not become merely an extension of spur gear action, but develops many specialized characteristics.

The nature of the oblique contact line shall be reviewed as it affects the following:

1. Contact action
2. Total length of oblique contact lines
3. Stress pattern
4. Load distribution
5. Elastic characteristics

1. The Contact Action

There is a characteristic difference between the mating of spur and helical teeth particularly in the transmission and transfer of load as the contact progresses along the line of action.

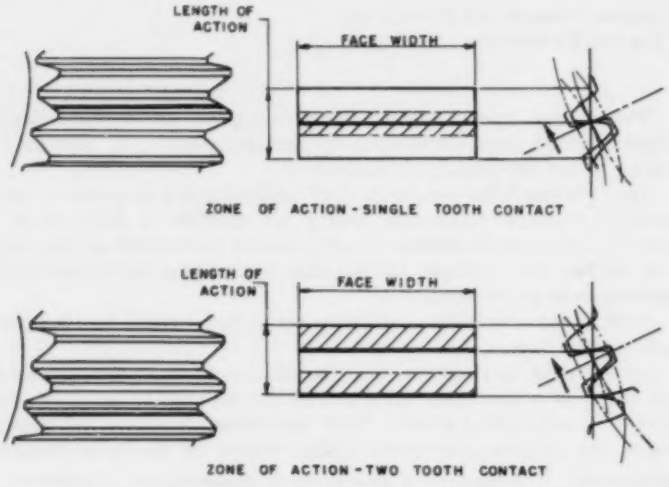
LENGTH OF ACTION
FACE WIDTH
ZONE OF ACTION - SINGLE TOOTH CONTACT
LENGTH OF ACTION
FACE WIDTH
ZONE OF ACTION - TWO TOOTH CONTACT

Fig. 2. Contact of Spur Gears.

Tooth action of spur gears normally results in either one or two teeth in contact. There can be no axial overlap of the lines of contact parallel to the axis. These characteristics are illustrated in

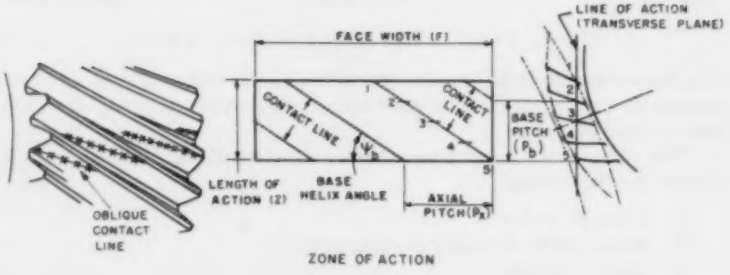

Fig. 3. Contact of Helical Gears.

Figure 2. In contrast, the helical gear usually has a multiple number of teeth in contact depending upon the geometric proportions. The lines-of-contact are oblique to the axis as shown in Figure 3. The geometric location of the oblique line is shown in Figure 4.

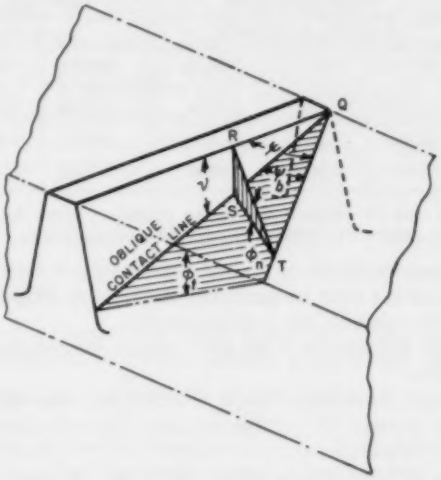

Fig. 4. Inclination Angle, ν of Oblique Contact Line.

Spur Tooth Load Transmission

The theoretical transmission and transfer of load for a spur gear is characterized by the load being shared alternately by one or two teeth for discrete portions of the tooth profile. Without proper accuracy load sharing between teeth is not possible and the load is abruptly transferred from one tooth to the next. Only one tooth is then in contact at any instance of action. Table 1 shows the accuracy required to insure load sharing.

The elastic flexibility is continuously changing throughout the contact cycle both because of the location of the load on the profile and also due to the fact that either one or two teeth are in contact.

Any error of spacing directly affects the uniformity of the angular velocity transmitted.

Helical Tooth Transmission

With a helical gear, profile contact can occur simultaneously along an oblique line extending from the beginning to the end of contact along the line of action.

Table I

Limiting Error in Action for Steel Spur Gears
(Variation in Base Pitch)

Number of Pinion Teeth	Allowable Error When Teeth Share Load			Amount of Error When Teeth Fail to Share Load		
	Load Per In. of Face			Load Per In. of Face		
	500 lb.	1,000 lb.	2,000 lb.	500 lb.	1,000 lb.	2,000 lb.
15	0.0004	0.0007	0.0014	0.0006	0.0011	0.0023
20	0.0003	0.0006	0.0011	0.0006	0.0011	0.0023
25	0.0002	0.0005	0.0009	0.0006	0.0011	0.0023

NOTE: When errors lie between the values indicated, more detailed studies or tests are required to determine the load sharing characteristics.

The load can be made to be shared between a sufficient number of teeth to allow the load to be more easily picked up by the incoming tooth and dropped by the outgoing tooth.

The elastic flexibility does not change measurably during the cycle of contact.

Spacing errors are less likely to affect uniform angular velocity because many phases of profile contact are simultaneously operating.

Conditions of abrasive wear do not cause excessive changes in the conjugate profile because accelerated wear along any portion of the oblique line-of-contact merely transfers the loading to another portion. Spur gears tend to depart from their conjugate profile more and more as abrasive wear or lapping proceeds because the highest lapping tendencies are concentrated in the position of the highest sliding. It is for this reason that helical gears can be successfully lapped and the statement is made "that helical gears can 'wear in' before 'wearing out'."

The total length of the contact developed between mating helical teeth is subjected to the effect of more variables than that of spur gears. A knowledge of these variables enables advantageous effects to be secured.

2. Total Length of Oblique Contact Lines

For accurate spur teeth, the total length of contact between mating profiles equals the face width when one tooth is in contact and twice the face width when two teeth are in contact.

For helical teeth the total length of contact along the oblique lines is a complex relationship between geometric dimensions,

particularly the ratio of face width to axial pitch (face contact ratio, m_F) and the ratio of the length of action in the transverse plane to the base pitch (profile contact ratio, m_p).

The minimum length of contact occurs when one of the oblique lines intersects and is external to the contact zone at the outer edge as shown at points W and Z in Fig. 5a. The maximum contact occurs when one of the contact lines intersects from the interior as shown at points K and Y, Fig. 5a.

The result is a discontinuous relationship which can be most easily solved by a criteria determination of certain parameters depending upon the fractional portions of the face contact ratio m_F and the profile contact ratio m_p.

Total Length of the Oblique Lines of Contact

NOTE: Attention is directed to these special notations which will be used in the following formulas:

K_a and n_a are the whole number and fractional portion respectively of the face contact ratio (axial overlap). For example, $m_F = \frac{F}{p_x} = 4.85$ then $K_a = 4.0$ and $n_a = 0.85$.

K_r and n_r are the whole number and fractional portion respectively of the profile contact ratio. For example, $m_p = \frac{Z}{p_b} = 1.32$ then $K_r = 1.0$ and $n_r = 0.32$.

K and K_m are the number of contact lines intersecting side K-Z of the contact zone (Fig. 5a) when a contact line intersects W or Y for L_{min} and L_{max} respectively.

L_{min} Calculation

The minimum total length of contact is obviously important because this is the condition which develops the maximum load intensity along the oblique contact lines and governs the profile durability (pitting resistance) and sometimes also the maximum bending stress. Its ratio to the maximum total length of contact has an important bearing on load capacity, mesh stiffness, etc.

The general equation for L_{min} is:

$$L_{min} = \frac{(K_a - K_r + K)(Z - Kp_b)}{\sin \psi_b} + \frac{KF}{\cos \psi_b} \qquad 1$$

Criteria equations useful for determining the value of K can be derived from Fig. 5b. The change from case I ($K = K_r$) to case II

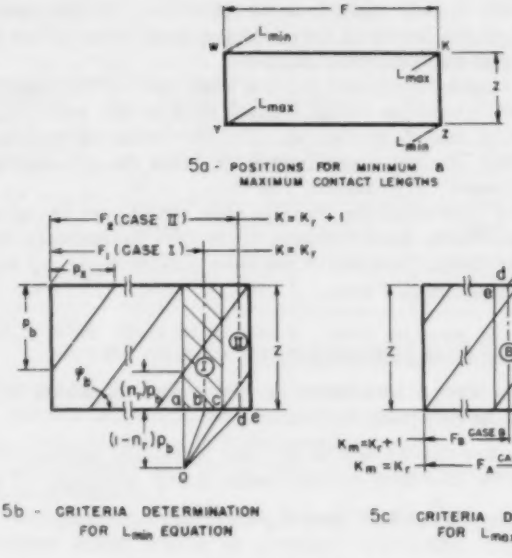

Fig. 5.

$(K = K_r + 1)$ occurs when the angle a o b equals and becomes greater than angle a o c. The change takes place when

$$(1 - n_r)\, p_b / n_a\, p_x = \tan \psi_b$$

or

$$\frac{1 - n_r}{n_a} = 1$$

Hence for:

Case I

$$\frac{1 - n_r}{n_a} \geq 1 \quad \text{then } K = K_r$$

and

$$L_{min} = \frac{(ZF/p_b) - n_r n_a p_x}{\cos \psi_b} \qquad 2$$

Case II

$$\frac{1 - n_r}{n_a} < 1 \quad \text{then } K = K_r + 1$$

and

$$L_{min} = \frac{(ZF/p_b) - (1 - n_a)(1 - n_r)\, p_x}{\cos \psi_b} \qquad 3$$

L_{max} Calculation

The maximum total length of the lines-of-contact is important because this often is the condition when the position of the worst tooth loading is secured in regard to bending strength and also is useful as a measure of the variation existing in the contact cycle. The general equation for L_{max} is:

$$L_{max} = \frac{(K_a + K_r + 1 - K_m)(Z - K_m\, p_b)}{\sin \psi_b} + \frac{K_m F}{\cos \psi_b} \qquad 4$$

Criteria equations for the determination of K_m can be derived from Fig. 5c similar to the procedure used for the criteria equations for K.

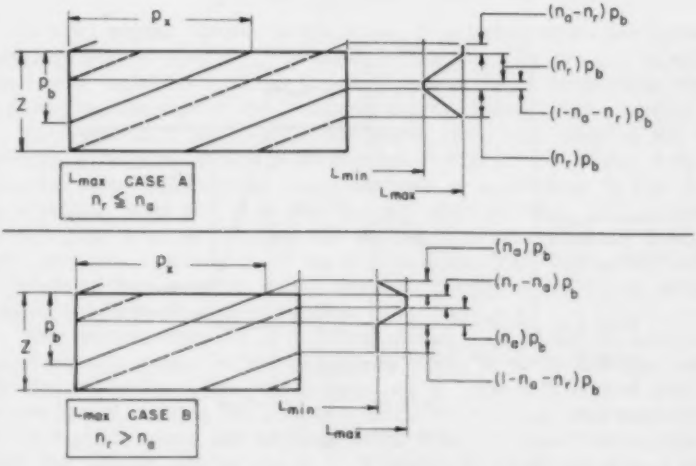

Fig. 6. Minimum Contact Length (L_{min}) — Case I ($1 - n_r \geqq n_a$)

Case A

$$n_r \leq n_a \quad \text{then } K_m = K_r$$

and

$$L_{max} = \frac{(ZF/p_b) + n_r (1 - n_a) p_x}{\cos \psi_b} \qquad 5$$

Case B

$$n_r > n_a \quad \text{then } K_m = K_r + 1$$

and

$$L_{max} = \frac{(ZF/p_b) + n_a (1 - n_r) p_x}{\cos \psi_b} \qquad 6$$

The mathematical relations for L_{min} and L_{max} existing through one base pitch movement of tooth contact along the length of the line of action in the transverse plane is illustrated by Fig. 6 and summarized for all cases in Fig. 7.

When either n_a or n_r is zero, in other words, if the ratios m_F

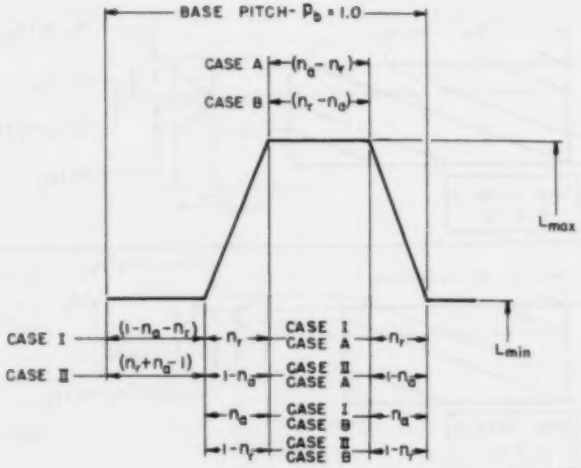

Fig. 7. Duration of L Through One Base Pitch Cycle.

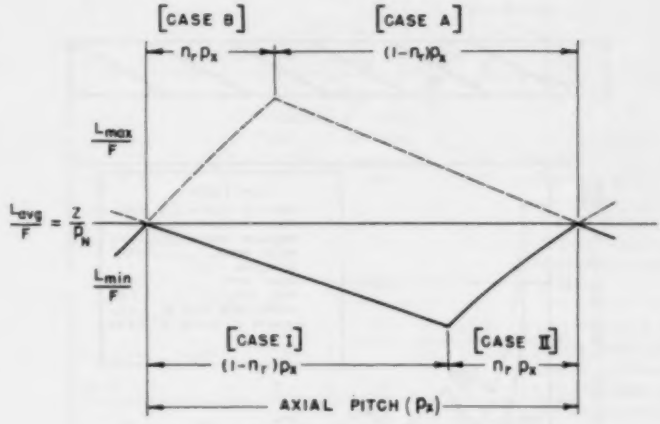

Fig. 8. $\frac{L}{F}$ Ratio vs Axial Overlap.

or m_p are whole numbers, then the contact length remains unchanged during all phases of the tooth contact cycle and is equal to

$$L = \frac{ZF}{p_N}$$

If the total contact length is integrated in relation to the period of duration (Fig. 7) then L_{avg} is equal to ZF/p_N. By general usage this has become known as the average contact length rather than the arithmetical average of the maximum and minimum contact lengths.

The ratio L/F as the face increases from one integral axial overlap to the next highest is illustrated in Fig. 8. The effect of increasing face contact ratio (axial overlap) is illustrated in Fig. 9. Of significance in Fig. 9 is the fact that the ratio L_{max}/L_{min} can be high when F/p_x is less than one but becomes progressively lower with increasing numbers of axial overlaps. The desirability of maintaining face contact ratios near an integer to minimize total contact length variations is evident.

This information has practical application in design as can be shown by the proportions compared in Table II. It is obvious that the changes in L_{min} are relatively small and the influence of pitch or number of teeth in the pinion is minor for the low ratio gear set of Example 1. When low numbers of teeth in the pinion are secured with the coarse pitches shown in Example 2, an appreciable loss in contact can be present. For the high ratio gear set shown in

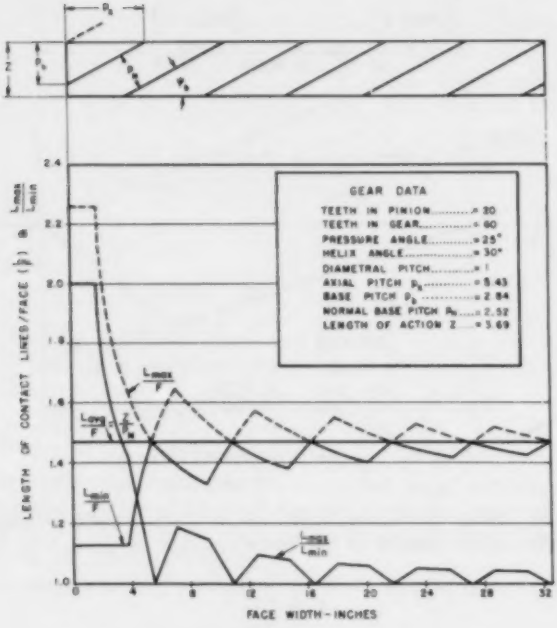
GEAR DATA
TEETH IN PINION = 20
TEETH IN GEAR = 60
PRESSURE ANGLE = 25°
HELIX ANGLE = 30°
DIAMETRAL PITCH = 1
AXIAL PITCH p_x = 5.43
BASE PITCH p_b = 2.84
NORMAL BASE PITCH p_n = 2.52
LENGTH OF ACTION Z = 5.69
LENGTH OF CONTACT LINES/FACE ($\frac{L}{F}$) & $\frac{L_{max}}{L_{min}}$
FACE WIDTH - INCHES

Fig. 9. Variation of $\frac{L}{F}$ Ratio with Face Width.

Example 3, a considerable percentage variation can exist in L_{min} depending upon the pitch selection. These comparisons demonstrate the importance of careful consideration for critical designs.

3. Stress Pattern

Bending Stress

A most significant difference exists between the stress pattern developed in spur and helical gear teeth because of the oblique line-of-contact. In the spur tooth with uniform load distribution the structure can be normally considered as a beam and the classical Lewis analysis applies.

With the oblique line-of-contact any approach using a beam analysis can result in serious error. The correct theory to use is that of a cantilever plate. According to the principles of a cantilever plate for any position of load the value of the maximum

Table II

Examples of L_{min} Variations

Example	Data	Diametral Pitch	Numbers of Teeth (Pinion)	L_{min} (in)	Remarks
1	m_g - 2.0 centers - 55½" face - 10"	1	37	14.8	Changes in L_{min} are relatively small and the influence of pitch or number of teeth in the pinion is minor
		2	74	15.1	
		3	111	15.8	
2	m_g - 2.0 centers - 15.0" face - 10"	1	10	12.5	Low numbers of pinion teeth with coarse pitches lead to a considerable percentage variation in total contact length
		2	20	13.9	
		3	30	14.6	
		4	40	15.1	
3	m_g - 10 centers - 55½" face - 10"	1	10	12.8	Even with high ratios L_{min} varies considerably depending upon pitch
		2	20	14.4	
		3	30	15.0	
		4	40	17.1	

moment at the fixed edge is independent of the absolute width of the plate or the absolute normal distance between the load and the fixed edge, being dependent only on the relative value of these dimensions. This is explained in the paper by Seireg and Wellauer (1).[1] The effect of the inclination angle on the moment distribution at the root is illustrated in Fig. 10.

It is evident that the "worst" position of loading for maximum stress can vary depending upon numerous conditions. Fig. 11 shows the moment distribution for various positions of the load line. The effect of buttressing and of change in load due to tooth end deflection or contact relief can also modify both the magnitude and the position of the maximum stress.

Contact Stress

The oblique line-of-contact also manifests its nature in regard to the contact stresses which determine the surface durability or

[1] Numbers in parentheses designate References at end of paper.

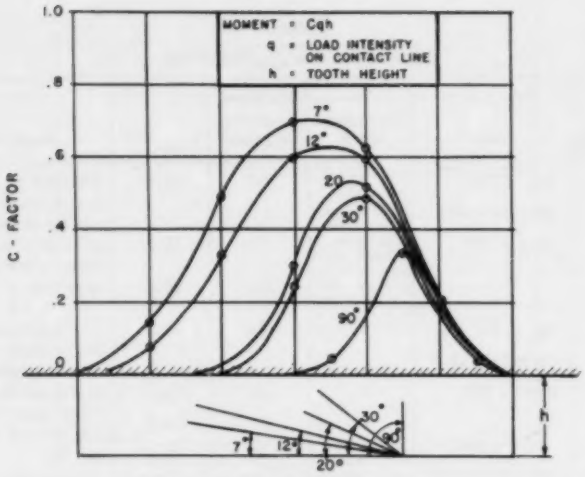

Fig. 10. Effect of Inclination Angle on the Moment Distribution at the Root (Load Line Away from the Corner).

resistance against pitting. Generally, spur gears can be considered as cylinders in contact whose relative diameters vary with the position of the contact along the profiles. The helical gear on the other hand must be considered as two truncated cones in contact.

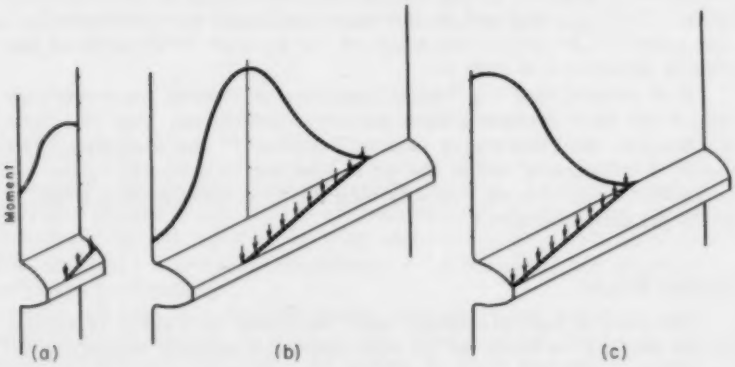

Fig. 11. Helical Gear Contact Conditions and Bending Moment.

This is a rather complex stress system which, as yet, has not been completely solved. The worst position for spur gears will be at that position of single tooth contact having the smallest relative radii of curvatures. On the other hand, for helical gears it is obvious that varying relative radii of contact exist simultaneously and experience alone has determined which value is important; this particularly because of the significant influence of elasticity on the distribution of the load.

The face of spur and helical gears are often crowned for better operation. The extension of the localized contact is proportionate to the cube root of the load for both types of gears.

4. Load Distribution

The load distribution between teeth and along the contact lines is very important. The oblique line-of-contact by virtue of its

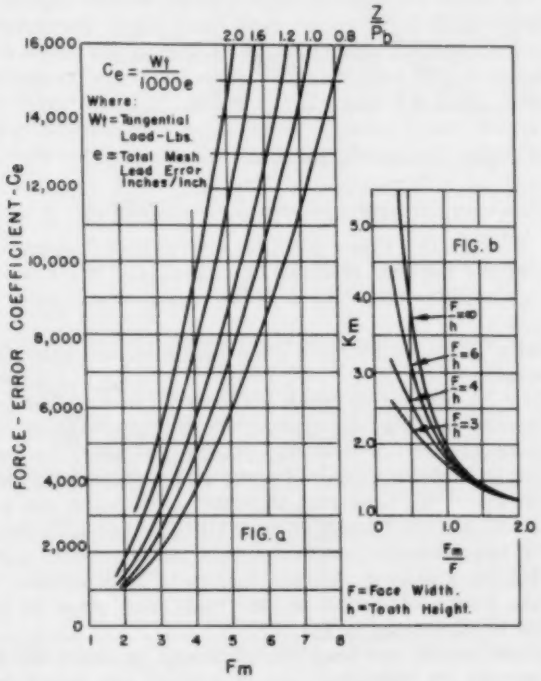

Fig. 12. Helical Gear Load Distribution Factor - K_m.

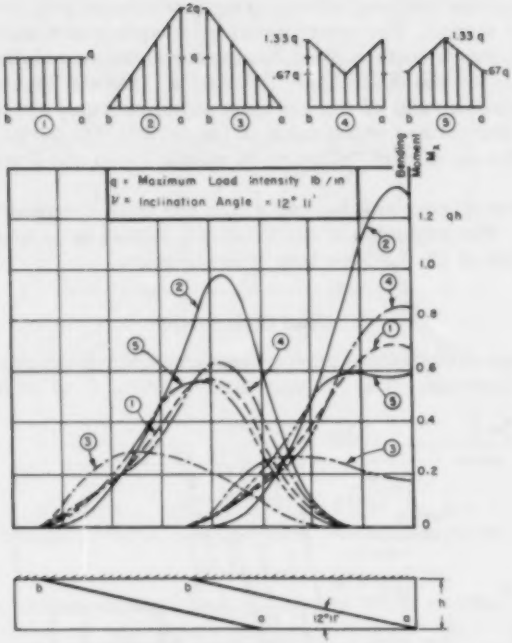

Fig. 13. Effect of Different Types of Loading on the Bending Moment Distribution at the Root of a Helical Gear with $12^{0}\,11'$ Inclination Angle.

contact action and uniformity of total length importantly affects the load distribution.

An effect is present on tooth deflection, the distribution of load along the individual lines-of-contact, the thermal expansion and the difference between cylindrical and conical contact. The analysis of the effect of tooth deflection is presented by Wellauer (2) and is primarily concerned with the fact that for spur gears the maximum rigidity affecting tooth contact is normally secured with two teeth in mesh. For helical gears, contact conditions are more uniform and the distribution of loading between two teeth is dependent upon the ratio of the length of action in the transverse plane to the base pitch. This is illustrated in Fig. 12.

Deliberate profile and lead modifications to affect the load distribution across an individual line-of-contact can result in variations of bending moment illustrated by Fig. 13.

5. Elastic Characteristics

The special elastic characteristics pertinent to the oblique line-of-contact of helical gears has practical significance both in regard to the performance of the blank and of the tooth. These phases involve vibration, dynamic loading and the width and depth of the flattened area.

Analyses of load sharing, deflection of teeth, and blank deflections are available in the literature.

Insofar as vibration is concerned, helical gears have been used almost universally for high pitch line velocities. There are several reasons for this preference. First, the smooth action previously discussed minimizes tooth excited forces and noise. Secondly, since the contact conditions are more uniform, there is less excitation due to the change of elastic mesh stiffness such as occurs with the one to two tooth load cycle in spur gears.

The oblique line-of-contact has an influence upon the dynamic loading developed by the gear teeth themselves. Fig. 14 based upon Harris (3) shows the derating expressed as a dynamic factor caused by the effects of base pitch errors and the load with reference to the pitch line velocity. Also plotted are commonly used velocity factors applied for rating commercial gears. Curves 1 and 2 are used for helical gears and precision spur gears whereas 3 and 4 have been

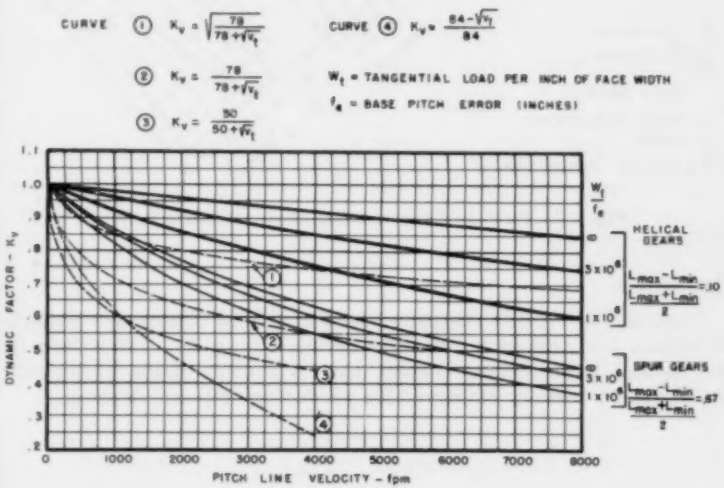
CURVE ① $K_v = \sqrt{\frac{78}{78+\sqrt{v_t}}}$
② $K_v = \frac{78}{78+\sqrt{v_t}}$
③ $K_v = \frac{50}{50+\sqrt{v_t}}$
CURVE ④ $K_v = \frac{84-\sqrt{v_t}}{84}$
W_t = TANGENTIAL LOAD PER INCH OF FACE WIDTH
f_a = BASE PITCH ERROR (INCHES)
DYNAMIC FACTOR - K_v
PITCH LINE VELOCITY - fpm
$\frac{W_t}{f_a}$
HELICAL GEARS
SPUR GEARS
$\frac{L_{max}-L_{min}}{\frac{L_{max}+L_{min}}{2}} = .10$
$\frac{L_{max}-L_{min}}{\frac{L_{max}+L_{min}}{2}} = .67$

Fig. 14. Variation of Dynamic Factor for Spur and Helical Gears.

used for less accurate spur gears. These curves follow the trend which might be predicted by the analyses.

It also is obvious that because of the helical shape, the metal in a helical gear blank is distributed more symmetrically around the cylindrical surface and opportunities for exciting lateral vibrations are at a minimum.

Fig. 15 is an example of the elastic contact deflections which can be obtained across the line-of-contact of helical gears. It is to be noted that the flattened land is of a significant width even for extremely minute deflections normal to the profile.

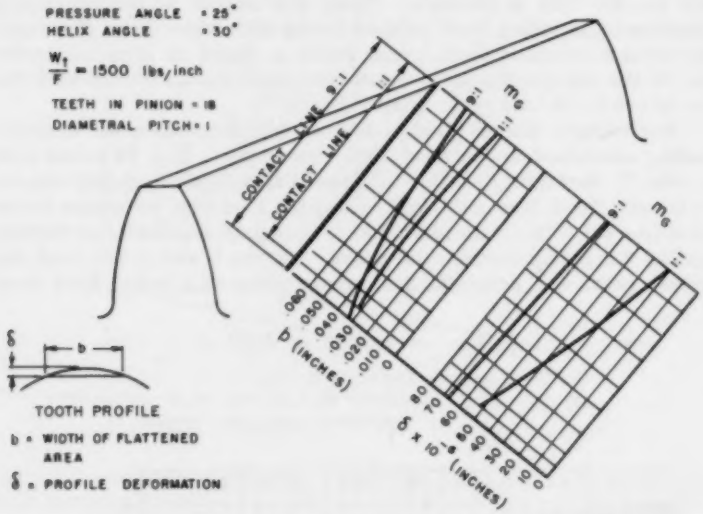

Fig. 15. Profile Deformation Along Contact Line.

Conclusion

Beside the factors discussed in this article others are equally important and sometimes deserve detailed analysis. The nature of the helical gear oblique contact line is a controllable parameter which can be usefully employed for producing optimum designs.

REFERENCES

1. Seireg and Wellauer - "Bending Strength of Gear Teeth by Cantilever-Plate Theory." Transactions of the ASME, Volume 82, Series B, Number 3, pp. 213-222, August, 1960, ASME, New York.

2. Wellauer - "An Analysis of Factors Used for Strength Rating Helical Gears" - Transactions of the ASME, Volume 82, Series B, Number 3, pp. 205-212, August 1960, ASME, New York.

3. S. L. Harris, "The Dynamic Loads in the Teeth of Spur Gears," Proceedings of the Institution of Mechanical Engineers, Volume 172, 1958, pp. 87-100.

2

Basic Geometry and Tooth Contact of Hypoid Gears

By Meriwether L. Baxter, Jr.
Chief Research Engineer
The Gleason Works
Rochester, New York

Basic Geometry of Hypoid Gears

There is no mystery about hypoid gears. There can hardly be any real mystery about a machine element that is produced in the millions each year by many unrelated companies; hypoid rear axle gears perform with quiet competence in vehicles all over the world.

The series of articles by Ernest Wildhaber in American Machinist in 1946 contains a complete description of the geometry and kinematics of hypoid gears; since the publication of the Wildhaber articles there has been a certain amount of correspondence with engineers in Europe and Japan indicating that they have made an intelligent study of at least parts of the series. There have been relatively few similar inquiries from American engineers, which perhaps indicates that the presentation was somewhat too general and too complete to appeal to the engineer with a production job to do.

This paper presents a simplified but logically complete description of hypoid geometry and kinematics which should clarify the meaning of the various terms encountered in hypoid design and calculation, and the relationships involved.

Synthesis of Hypoid Geometry

Our geometry contains at the beginning two axes in space; in general they do not intersect, and are neither parallel nor orthogonal. Now we can define a new line which is the common perpendicular to the two axes, called the *line of centers*. The distance

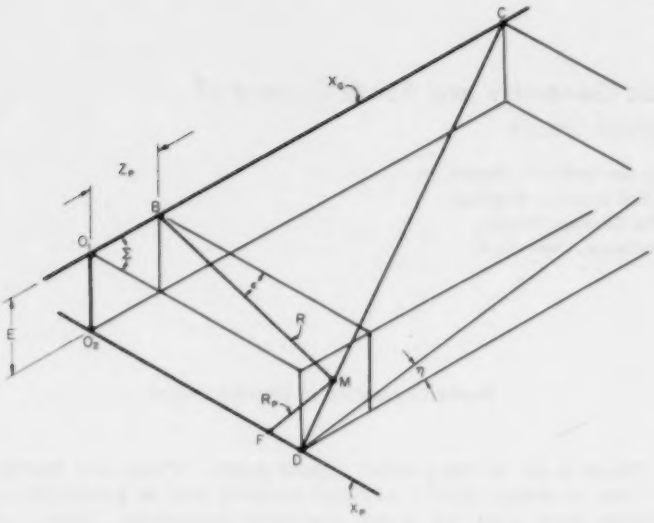

Figure 1.

between the two axes measured along the line of centers is the *offset* E. Figure 1 shows the axes X_G and X_P and the line of centers $\overline{O_1 O_2}$. The angle between the axes is naturally measured in a plane parallel to both, and its symbol is Σ. For definiteness we shall call X_G the gear axis and X_P the pinion axis.

We now propose to transmit motion from one axis to the other by direct tangent contact between a pair of surfaces, that is, by gear teeth; and it is clearly necessary to make a decision as to where in our space the contact is to take place. This decision is a critical one, and determines the kind of gears we shall end up with. Special cases yield special results; for example if the tooth mesh is to take place on the line of centers we shall obtain worm gears. Since hypoid gears are the most general kind of gear, we must choose a general point, such as M in Figure 1.

The mean point M can be specified in a variety of ways; we choose to locate it by the three quantities, R, ϵ, and Z_P shown in the figure. It will be seen that Z_P specifies the plane of rotation of the gear in which M lies; that R is the mean radius of the gear; and that ϵ gives the orientation of M in its plane of rotation.

Through M we can construct line $\overline{CD}$ intersecting both axes; this line is called the *pitch vertical* and is an important element in our geometry. It will be seen that the inclination of the pitch vertical

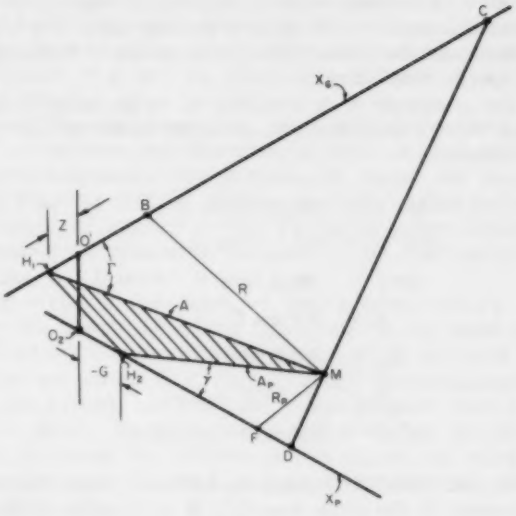

Figure 2.

when viewed along the gear axis X_G is the given angle ϵ; similarly the angle η is the inclination of the pitch vertical when viewed along the pinion axis.

R_P is the distance of mean point M from the pinion axis; that is, the mean pinion radius. In the material that follows we shall assume the axes to be at right angles in order to simplify formulas and diagrams; the principles however are general.

From the geometry of Figure 1 the formulas for the newly defined quantities η and R_P are as follows:

$$\tan \eta = \frac{1}{Z_P} (E - R \sin \epsilon) \tag{1}$$

$$R_P = Z_P \sec \eta \tag{2}$$

Let us now consider a plane containing mean point M and perpendicular to the pitch vertical. Figure 2 shows such a plane, intersecting the gear axis at H_1, the *gear apex*, and the pinion axis at H_2, the *pinion apex*. For reasons to be seen later we shall call this the *pitch plane*, the distance $\overline{MH_1}$ the *gear cone distance* A, and the distance $\overline{MH_2}$ the *pinion cone distance* A_P. Likewise the angle between the gear axis and the pitch plane is the *gear pitch angle* Γ, while

the pinion axis is inclined at the *pinion pitch angle* γ to the pitch plane. Other quantities to be defined are the angle $\epsilon' = \sphericalangle H_1 M H_2$ in the pitch plane and the linear dimensions Z and G locating the gear and pinion apices respectively.

From the geometry it is possible to write many relationships between our defined quantities; those listed below are sufficient and relatively simple

$$\tan \gamma = \sin \eta \operatorname{ctn} \epsilon \tag{3}$$

$$\cos \Gamma = \sin \gamma / \cos \epsilon \tag{4}$$

$$\sin \epsilon' = \sin \epsilon / \cos \gamma \tag{5}$$

$$A = R / \sin \Gamma \tag{6}$$

$$A_P = R_p / \sin \gamma \tag{7}$$

$$Z = A \cos \Gamma - Z_P \tag{8}$$

$$G = -R \cos \epsilon + A_P \cos \gamma \tag{9}$$

Since the pitch vertical intersects both axes, and the pitch plane is perpendicular to the pitch vertical, it is possible to describe a

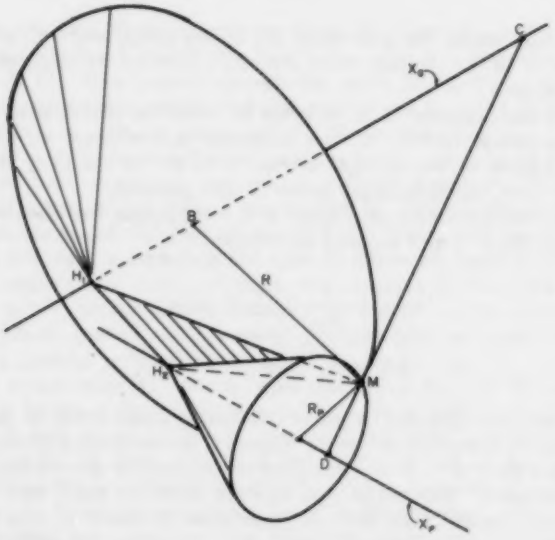

Figure 3.

pair of cones, one about each axis, which are tangent to each other at M. The apex of the gear cone is at H_1 and that of the pinion cone is at H_2; the lengths of the conical elements to the mean point M are the cone distances A and A_P previously defined. Figure 3 shows these pitch cones.

It should be emphasized that these pitch cones are not "pitch surfaces" in the sense that this term is used for gearing with parallel or intersecting axes. For example, we cannot say that the pitch cones roll together without sliding, since up to this point we have not introduced the velocity ratio. The pitch cones should be considered merely as geometric elements to be used as the basis of design of the gear blanks.

To summarize to this point, we have started with a pair of axes related by the quantities E, the offset, and Σ, the shaft angle. We then assumed the location of a mean point M of the tooth mesh, defined by the quantities R, ϵ, Z_P. Through the mean point we have defined a pitch plane, and two pitch cones tangent to each other and to the pitch plane. We have determined formulas for the pertinent quantities, including the location of the apices, the cone distance, the pitch angles, and the angle ϵ' in the pitch plane between the two cone elements.

Velocity Ratio Determines Spiral Angles

Figure 4 is a view of the pitch plane; we are looking along the pitch vertical from the pinion axis toward the gear axis; H_1 and H_2 are the gear and pinion apices respectively. The gear pitch cone lies below the view, and the pinion pitch cone above. The vector $\bar{g}$ is a unit vector in the direction of the gear axis; associated with it is the gear angular velocity ω_G. Similarly vector $\bar{p}$ has the direction of the pinion axis and is associated with the angular velocity ω_p. Vectors $\overline{A}$ and $\overline{A_p}$ run from the apices to the mean point M; their magnitudes are the cone distances A and A_p.

The vector velocity of M considered as a point on the gear is

$$\overline{V_G} = \omega_G \, \bar{g} \times \overline{A} \tag{10}$$

and its magnitude is $A \sin \Gamma \cdot \omega_G$. Similarly for the pinion

$$\overline{V_P} = \omega_p \, \bar{p} \times \overline{A_p} \tag{11}$$

of magnitude $A_p \sin \gamma \cdot \omega_p$. Due to the assumption of direction chosen for $\bar{p}$ and $\bar{g}$, the relative velocity vector may be written

$$\overline{V} = \overline{V_G} + \overline{V_P} = \omega_G \, \bar{g} \times \overline{A} + \omega_p \, \bar{p} \times \overline{A_P} \tag{12}$$

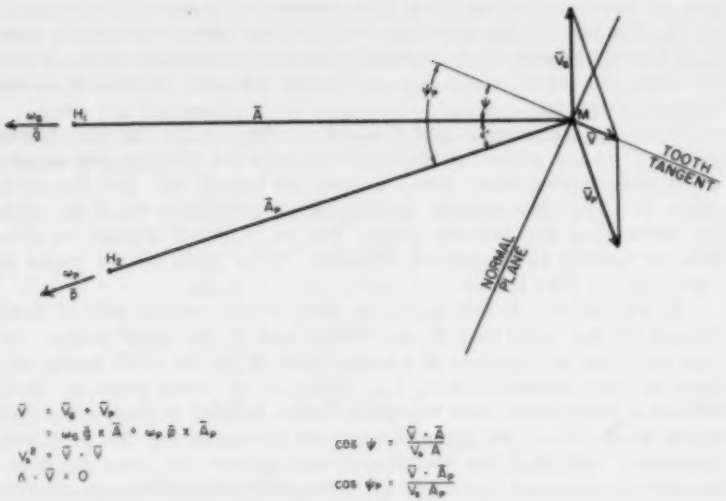

Figure 4.

The relative velocity vector $\overline{V}$ lies in the pitch plane, and serves to determine the tooth direction. If tooth contact is to take place at M with the specified velocity ratio the fundamental law of gear tooth contact must hold: the relative normal velocity must be zero. This law is expressed very simply in vector notation

$$\overline{V} \cdot \overline{n} = 0 \tag{13}$$

where $\overline{V}$ is the relative velocity vector and $\overline{n}$ is a vector along the common contact normal.

As seen in Figure 4, we define the gear spiral angle ψ as the angle between the tooth tangent and the gear pitch cone element, and the pinion spiral angle ψ_p as the angle between the tooth tangent and the pinion pitch cone element.

The sliding velocity for contact at M is the magnitude of vector $\overline{V}$ and can be calculated by

$$V_s = \sqrt{\overline{V} \cdot \overline{V}} \tag{14}$$

The spiral angles may be obtained from

$$\cos \psi = \frac{\overline{V} \cdot \overline{A}}{V_s A} \tag{15}$$

$$\cos \psi_p = \frac{\overline{V} \cdot \overline{A_p}}{V_s A_p} \tag{16}$$

The more familiar algebraic formulas are

$$\frac{\cos \psi}{\cos \psi_p} = \frac{A_p \sin \gamma}{A \sin \Gamma} \cdot \frac{N}{n} = \frac{R_p}{R} \cdot \frac{N}{n} \tag{17}$$

$$\psi_p = \psi + \epsilon' \tag{18}$$

$$V_s = R \omega_G \cos \psi (\tan \psi_p - \tan \psi) \tag{19}$$

The tooth normal may have any direction perpendicular to $\overline{V}$ or the tooth tangent; thus the pressure angle is subject to free choice. The spiral angles however are fixed by the chosen mean point and velocity ratio. If the spiral angles are not satisfactory we must change one of the assumptions for the location of the point M; usually Z_p is changed for this purpose.

Surfaces of Action

Within reason we can choose any tooth shape for one member, say the gear, and the conjugate surface for the mate and the surface of action can be determined. If the chosen mean point M is to lie in the surface of action the direction of the tooth tangent must of course be as calculated above.

The suitability of a particular tooth shape can be studied by reference to its surface of action. The relationship between the path of action and such conditions as undercut and contact ratio is well understood, and it is natural that similar considerations should govern the choice of tooth surfaces and surfaces of action for hypoid gears. In particular we may wish to specify (a) that the two surfaces of action be equally inclined to the pitch plane, and (b) that the two surfaces of action intersect in a line tangent to the pitch plane.

The first of these aims is intended to produce equal contact ratio and equal freedom from undercut for the two sides of the teeth. For good reason we sometimes wish to depart from this balanced condition, but to do this intelligently we must first know how to get the balance. Failure to meet the second requirement at least approximately will result in teeth which are pointed at one end and undercut at the other.

$$\overline{\Delta A} = \overline{\Delta A_p} = \theta\, \bar{g} \times \bar{A}$$

$$\overline{\Delta V} = (\omega_G\, \bar{g} + \omega_p\, \bar{p}) \times \overline{\Delta A}$$

$$\overline{\Delta n} = \theta\, \bar{g} \times \bar{n}_o$$

$$\bar{V} \cdot \overline{\Delta n} + \overline{\Delta V} \cdot \bar{n}_o = 0$$

$$\begin{cases} \bar{n}_o \cdot [\bar{g} \times (\bar{g} \times \bar{A}) - \bar{g} \times (\bar{p} \times \bar{A}_p)] = 0 \\ \bar{n}_o \cdot \bar{V} = 0 \end{cases}$$

$$-\tan \phi_o = \frac{A_p \sin \psi_p - A \sin \psi}{A_p \tan \gamma + A \tan \Gamma}$$

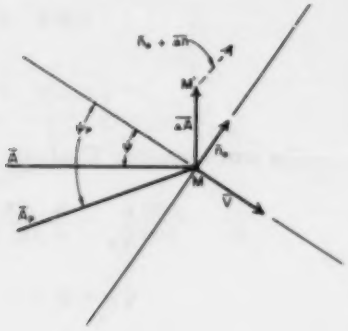

Figure 5.

Due to the shaft offset of hypoid gears an unsymmetrical condition exists such that the surface of action makes an angle with the pitch plane which is not equal to the pressure angle of the tooth surface. In fact there is a particular hypoid pressure angle, called the "limit pressure angle" which produces a line in the surface of action tangent to the pitch plane, and which therefore may be said to be equivalent to zero pressure angle for other types of gears.

Figure 5 is similar to Figure 4, and shows a unit normal vector to the gear tooth, $\bar{n}_o$, inclined to the pitch plane at the limit pressure angle ϕ_o. As the gear rotates through a small angle θ, point M of the gear is carried to M', where

$$\overline{MM'} = \overline{\Delta A} = \theta\, \bar{g} \times \bar{A} \tag{20}$$

$$\overline{\Delta A_p} = \overline{\Delta A} \tag{21}$$

The change in $\bar{n}_o$ due to rotation θ is

$$\overline{\Delta n} = \theta\, \bar{g} \times \bar{n}_o \tag{22}$$

If M' is to remain a point of contact, then the formula $\bar{V} \cdot \bar{n} = 0$ must continue to be fulfilled, or

$$\bar{V} \cdot \overline{\Delta n} + \overline{\Delta V} \cdot \bar{n}_o = 0 \tag{23}$$

Differentiating equation (12) we obtain

$$\overline{\Delta V} = \omega_G\, \bar{g} \times \overline{\Delta A} + \omega_p\, \bar{p} \times \overline{\Delta A_p} \tag{24}$$

Substituting from equations (12), (20), (21), (22), (24) in equation (23) gives

$$(\omega_G \bar{g} \times \bar{A} + \omega_p \bar{p} \times \bar{A_p}) \cdot (\theta \bar{g} \times \bar{n_0}) + (\omega_G \bar{g} + \omega_p \bar{p}) \times (\theta \bar{g} \times \bar{A}) \cdot \bar{n_0} = 0$$

which can be simplified to

$$\bar{n_0} \cdot [\bar{p} \times (\bar{g} \times \bar{A}) - \bar{g} \times (\bar{p} \times \bar{A_p}] = 0 \qquad (25)$$

This is sufficient to define the limit pressure angle ϕ_0.

The equivalent algebraic formula for ϕ_0 is

$$-\tan \phi_0 = \frac{A_p \sin \psi_p - A \sin \psi}{A_p \tan \gamma + A \tan \Gamma} \qquad (26)$$

This value of θ_0 is regularly used in hypoid design to determine the amount of unbalance for the gear tooth pressure angles.

Now let us assume a gear tooth of the limit pressure angle θ_0 to be a surface of revolution about an axis perpendicular to the pitch plane, as seen in Figure 6. Unit vector $\bar{c}$ is directed along the axis of revolution, and a vector $(r_{n_0} \bar{n_0})$ connects the axis to mean point

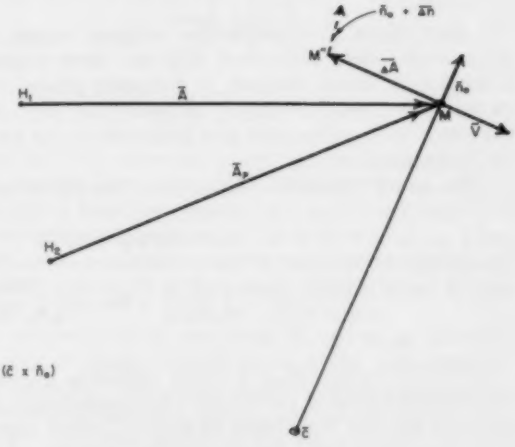

$$\bar{\Delta A} = \theta \bar{c} \times r_{no} \bar{n}_0$$

$$\Delta \bar{n} = \theta \bar{c} \times \bar{n}_0$$

$$\bar{\Delta V} = (\omega_G \bar{g} + \omega_p \bar{p}) \times r_{no} \theta (\bar{c} \times \bar{n}_0)$$

$$= r_{no} \theta \bar{\omega} \times (\bar{c} \times \bar{n}_0)$$

$$\bar{\Delta V} \cdot \bar{n_0} + \bar{V} \cdot \bar{\Delta n} = 0$$

$$r_{no} = -\frac{V_a^2}{\bar{n}_0 \cdot (\bar{\omega} \times \bar{V})}$$

$$(r_{no} \cos \phi_0) = \frac{\tan \psi_p - \tan \psi}{\frac{1}{A_p \cos \psi_p} - \frac{\because 1}{A \cos \psi} - \tan \phi_0 \left(\frac{\tan \psi_p}{A_p \tan \gamma} + \frac{\tan \psi}{A \tan \Gamma}\right)}$$

Figure 6.

M. If we rotate M about $\bar{c}$ to a new point M", the latter point remains on the tooth surface and in the pitch plane. If the angle of rotation is θ,

$$\overline{\Delta A} = \theta\, \bar{c} \times r_{no}\, \overline{n_o} \tag{27}$$

$$\overline{\Delta n} = \theta\, \bar{c} \times \overline{n_o} \tag{28}$$

as before, $$\overline{\Delta V} = (\omega_G\, \bar{g} + \omega_p\, \bar{p}) \times \overline{\Delta A} \tag{29}$$

and $$\overline{\Delta V} \cdot \overline{n_o} + \bar{V} \cdot \overline{\Delta n_o} = 0 \tag{30}$$

By substitution, as above

$$(\omega_G\, \bar{g} + \omega_p\, \bar{p}) \times (\theta\, r_{no}\, \bar{c} \times \overline{n_o}) \cdot \overline{n_o} + \bar{V} \cdot \theta\, \bar{c} \times \overline{n_o} = 0 \tag{31}$$

If we let $(\omega_G\, \bar{g} + \omega_p\, \bar{p}) = \bar{\omega}$ = the relative angular velocity, then this relation reduces to

$$r_{no} = -\frac{V_s 2}{\overline{n_o} \cdot (\bar{\omega} \times \bar{V})} \tag{32}$$

Thus there is a particular normal radius of curvature of the gear tooth which when used with the limit pressure angle produces a surface of action tangent to the pitch plane. Since θ_o is in effect an average pressure angle between the two sides, the radius of curvature thus calculated is a good choice for real teeth of ordinary pressure angle.

The usual algebraic formula for the limit radius of curvature is

$$(r_{no} \cos \phi_o) = \frac{\tan \psi_p - \tan \psi}{\dfrac{1}{A_p \cos \psi_p} - \dfrac{1}{A \cos \psi} - \tan \phi_o \left[\dfrac{\tan \psi_p}{A_p \tan \gamma} + \dfrac{\tan \psi}{A \tan \Gamma}\right]} \tag{33}$$

In order to arrive at a limit radius of curvature corresponding to a standard size of cutter used for manufacturing hypoid gears, we can vary the assumed value of angle ϵ, which was one of the parameters originally used to specify the location of the mean point M, just as we varied the assumed value of Z_p to obtain suitable spiral angles. While this trial-and-error procedure sounds cumbersome it is not difficult in practice, and a satisfactory design can be achieved in a short time with the use of a desk calculator.

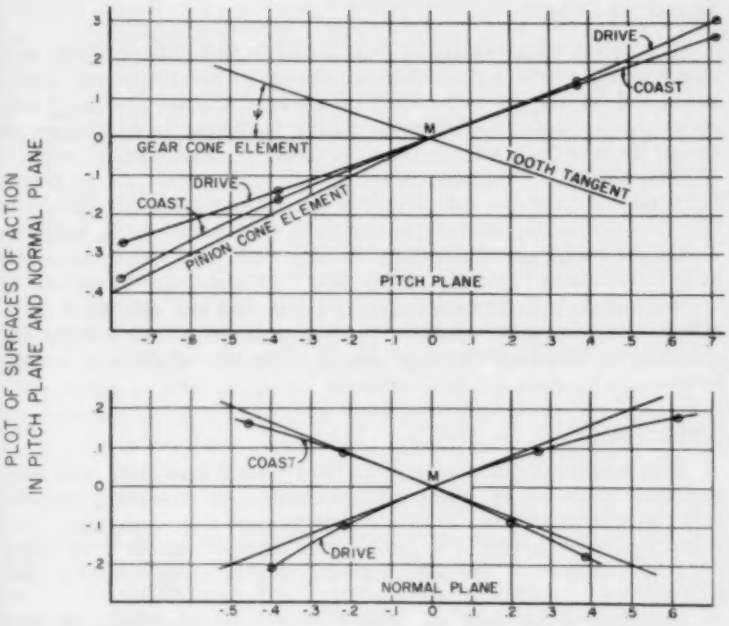

Figure 7.

It is of course possible to calculate actual points in the surface of action for a particular tooth surface. To demonstrate the effectiveness of the concepts of limit pressure angle and limit radius of curvature, we have calculated these values for a typical automotive hypoid ratio; we have chosen pressure angles unbalanced by exactly the limit pressure angle, and radii of curvature exactly equal to the limit value.

Figure 7 shows the trace of the surfaces of action in both the pitch plane and the normal plane. It will be seen that the surfaces of action are only moderately curved, and that the pitch-plane traces lie close together, indicating that the intersection of the surfaces of action lies very close to the pitch plane. In the normal plane we see that the lines of action are well balanced for direction.

These results justify the use of the limit pressure angle and the limit radius of curvature as basic design parameters for ordinary cases. In extreme cases of offset, ratio, or spiral angle we do of course make a detailed study of the actual surfaces of action.

Mismatched Gears

A primary requirement of real gears is that they perform well under actual operating conditions. Owing to manufacturing tolerances and deflections under load, gear and pinion are seldom if ever operating in their theoretical relative positions; nevertheless we expect them to transmit the required power smoothly and quietly.

Theoretically conjugate bevel and hypoid gears can be manufactured, but they are not practical because of their sensitivity to the misalignments inherent in any real gear housing. In order to obtain the required adjustability we introduce into the teeth of one or both members carefully chosen modifications usually referred to as "mismatch." By properly choosing the kind and amount of mismatch best suited to a particular application, we obtain results far superior to those which would result from theoretically conjugate teeth.

Tooth Bearing

It is a general practice to judge the type and amount of mismatch in a pair of gears by running them together in a testing machine under light load with the tooth surfaces painted with a marking compound such as red lead. The resultant marking on the tooth is called the "tooth bearing." The shaded area in Figure 8 represents a tooth bearing.

Correctly made teeth will show a tooth bearing centrally located on the tooth surface, when the gears are run in their standard relative positions. The amount of lengthwise mismatch is readily observed by the length of the tooth bearing; under light load the bearing will frequently cover about one half of the face width. Profile mismatch is not observed as readily owing to the fact that the tooth height is relatively small; nevertheless the existence of profile mismatch is evidenced by the lack of any heavy concentration of bearing at the tips of the teeth.

By displacing the pinion specified amounts on the testing machine we observe the resultant movement of the tooth bearing, and are then able to judge the adequacy of the set to operate in its particular application. "Development" of a gear pair is the process of generating pinions with a variety of combinations of mismatch to determine the one best suited to the job.

The testing machine adjustments which have been usually used in the past to displace the bearing are a change in the running offset and a change in the pinion axial position. The former is frequently called a "vertical" change and represented symbolically by V. The latter is called "horizontal" change and represented by H. The combined V-and-H change required to cause the tooth bearing to

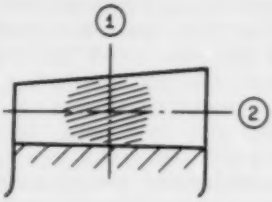

Figure 8.

Figure 9.

move from one end of the teeth to the other while remaining at an average height on the profile is called the "V-and-H check" and is frequently used to characterize the over-all nature of a particular tooth contact. This is frequently written in the form of a fraction; for example

$$\frac{V}{H} = \frac{21}{15}$$

means that a combined change of 0.021 in. vertical adjustment and 0.015 in. of horizontal adjustment on the testing machine will move the tooth bearing from toe to heel, while maintaining a good profile position. However, these figures do *not* indicate the amount of individual vertical or horizontal adjustment which can be tolerated.

The tooth bearing also serves to detect the existence of a contact condition known as "bias" in which the tooth bearing extends in a diagonal direction across the tooth. Some degree of bias is sometimes introduced to obtain a quieter job, or to produce a different V/H ratio. Like lengthwise and profile mismatch, bias can be readily controlled by alterations in the setting used to generate the pinion.

Newer designs of testing machines use a change in shaft angle instead of the vertical to accomplish a shift in bearing from end to end.

By listening to the gears in the testing machine, observing the position and shape of the tooth bearing, and observing the direction and amount of tooth-bearing movement under displacement, it is possible to develop a gear pair tailored to the particular requirements. The method in general is not however entirely satisfactory for the following reasons:

1. It is relatively costly and time-consuming.
2. Personal judgment is an important factor.
3. It provides little basis for further investigation.

For these reasons we have developed an analytical method for determining quantitatively the conditions of contact and motion transmission in mismatched gears; this has been called TCA (tooth contact analysis).

Brief Description of TCA

TCA permits us to calculate the tooth-bearing characteristics for a bevel or hypoid gear pair in any specified running position; in addition, it provides graphs of the transmitted motion. Thus to some degree it replaced conventional development using the testing machine.

On the other hand it is entirely theoretical, and does not at present consider such important practical matters as bending and compression of teeth under load, or distortion due to heat-treatment. For this reason TCA should be considered a supplement to and not a replacement of traditional methods. An important advantage however is that it provides a sound theoretical basis for further research in the subject of gear tooth action now being carried on at the author's company.

The data required for TCA are simply the machine settings used to manufacture gear and pinion, and the specified running position of the pair (not necessarily the nominal running position).

The results of TCA are as follows:

1. Data for plotting the tooth bearing.
2. Data for plotting motion graphs.
3. Calculated V-and-H check.

Calculated results of TCA correlate well with observed results under light loads in the testing machine; moreover, rather small changes which would be difficult for a machine operator to set or observe produce definite and repeatable effects.

Qualitative Description of Tooth Contact

In order to establish a theoretical basis for the study of tooth contact it is first necessary to arrive at a description of what actually takes place as gear teeth mesh together with combined rolling and sliding action. To this end we first discuss conjugate gears, and then show the effects of mismatch.

Fully Matched Gears

Let us consider real gears rotating about fixed axes with a constant velocity ratio, and equally spaced identical teeth.

We may take any reasonable surface as the tooth surface for one member and determine the conjugate surface for the other member, such that (a) the velocity ratio is maintained, (b) there is line contact within the physical boundaries of the tooth surfaces.

As rotation proceeds, the line of contact progresses across the tooth surfaces of both members, usually changing direction and shape as it does so. The angle of rotation during which a particular line of contact exists is determined by the tooth boundaries, and is greater than one pitch in properly designed gears. The ratio of this angle to the angular pitch is known as the "contact ratio."

Figure 9 shows a tooth surface and the successive positions of the line of contact. The solid lines represent two positions separated by a rotation of one pitch. The ratio of the number of lines encompassed by the tooth surface to the number for one pitch is the total contact ratio.

Figure 10 is a motion graph for conjugate teeth. The ordinate represents error in position of the driven member, zero in this case. The abscissa represents rotation of the driver. It will be seen that the action of successive teeth overlap and that there are two teeth in contact during the shaded intervals. This can occur because the velocity ratio is constant.

Single Mismatch

Now consider the tooth surface in Figure 11. This surface was obtained by starting with the tooth in Figure 9 (which was conjugate to its mate) and relieving it on both sides of line AB in such a way that the surface remains continuous and tangent to the original surface along line AB.

As this tooth meshes with the mating member, there will be a position where the line of contact with the conjugate member was

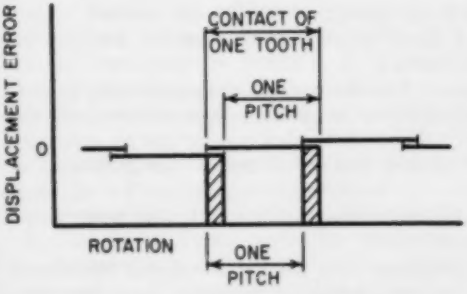

Figure 10.

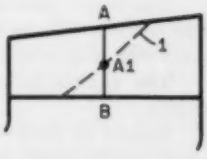

Figure 11.

at (1). Now, however, only point A1 can be in contact, since all other points on the line of contact have been relieved. Since point A1 is a point of the original surface, the position of the driven member relative to the driver is correct. Therefore:

1. There will be point (not line) contact.
2. Uniform velocity will be maintained.
3. The path of the contact point is line AB.

Figure 10 is also a correct motion graph for single mismatch.

Combined Mismatch

Most spiral bevel and hypoid gears are relieved both profilewise and lengthwise, so that only a single point in the center of the tooth is unchanged from the theoretically conjugate surface. Combined mismatch permits the gear pair to tolerate displacements under load and assembly errors.

With combined mismatch, as with single mismatch, there is theoretically point contact at any instant, and a path of contact across the teeth. However, the velocity ratio will not remain constant, and there is a theoretical instantaneous velocity change at each tooth changeover which is of interest to us analytically although its actual effect will be largely damped-out under load.

It is the purpose of TCA to reveal the contact conditions for combined-mismatch teeth.

Motion Curves for Combined Mismatch

The upper part in Figure 12 is the same kind of graph as Figure 10. We have plotted the error in displacement of the driven member against rotation of the driver for the entire duration of contact for one pair of teeth, as though no other teeth existed.

As would be expected, the driven member lags behind its correct position except at one instant.

The lower part in Figure 12 is the corresponding velocity curve. The velocity of the driven member is greater than standard at the start and less at the end.

The curves in Figure 12 are typical of teeth with profile mismatch.

Figure 13 shows the motion curves in Figure 12 with successive tooth meshes superimposed.

The intersection of the successive displacement curves is the "transfer point" at which contact shifts from one tooth to the next. The transfer points are one pitch apart.

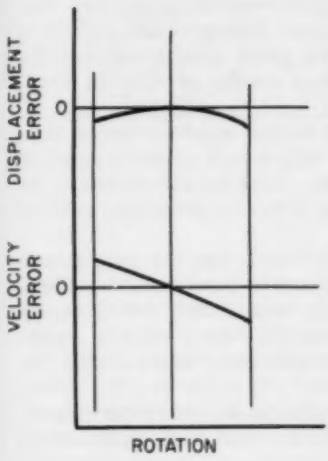

Figure 12.

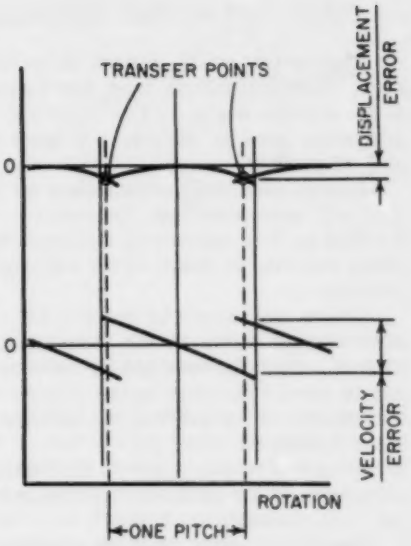

Figure 13.

The portions of the displacement curves beyond the transfer point are therefore not used, but their length is an indication of the amount of extra contact area available on the teeth to provide adjustability and accommodate misalignment.

The displacement error at the transfer point is the theoretical amount the driven member oscillates with each tooth mesh. This is usually a few tenths of a thousandths of an inch.

The velocity curves in Figure 13 do not intersect; at the transfer points there is a sudden jump in the velocity of the driven member, which is the velocity with which the new driving tooth strikes its mate. This value is therefore a measure of the impact occurring at each tooth mesh.

As profile mismatch is increased, the impact and oscillations increase in magnitude, resulting in noise and stress. It is therefore essential that mismatch be kept to the smallest value compatible with the adjustability requirements.

It should be emphasised again that these motion errors are only theoretical concepts useful for analysis and research, and that the real motion transmitted will be essentially uniform due to the averaging effect produced by the application of a load, and its resulting deflections.

Contact Mark and Tooth Bearing for Combined Mismatch

Theoretical point contact is, of course, only an imaginary concept. Under even light load, tooth surfaces compress and deflect to cause surface contact. Furthermore, the grain size of any marking compound used is sufficient to show area contact around the theoretical point of contact.

It has been found that gears on a testing machine under light load will show marking wherever the surfaces are closer than about 0.00025 in. (one quarter of a thousandth). Thus we can calculate the shape and size of mark which will show around a particular point of contact.

These contact marks are roughly elliptical, with the long axis in about the direction of the lines of contact of the conjugate gears. Their length is determined by the amount of mismatch. Such marks can be observed easily on the testing machine with a suitable marking compound by holding one member stationary and rocking the mate against it.

As gears roll together in the testing machine, the contact marks move across the tooth surfaces to produce a total marking known as the tooth bearing.

Figure 14 shows how we may indicate the calculated bearing. Points T1 and T2 are points of contact corresponding to transfer, and the path of contact is indicated as a slightly curved line between T1 and T2.

The elliptical contact marks have been indicated for points T1 and T2 and for another contact point in between.

The theoretical tooth bearing, therefore, is bounded as follows:

A = portion of contact ellipse for T2.
B = deepest contact of teeth of mate.
C = envelope of ends of contact ellipses.
D = portion of contact ellipse for T1.
E = tip of tooth.
F = envelope of ends of contact ellipses.

In the case shown in Figure 14, the entire path of action from transfer point to transfer point lies on the tooth surface. Therefore, we do not expect the marking at E and B to be particularly heavy.

In Figure 15, we have a case where one transfer point, T1, lies outside of the tooth boundaries. As contact moves from T2 to X, conditions are similar to those in Figure 14. Beyond X, however, motion must be transmitted by the edge of the tooth E to the left of X, resulting in a heavy edge contact line and a distortion of the

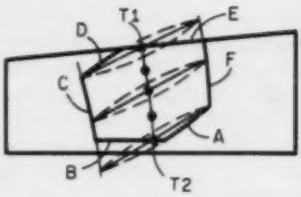

Figure 14.

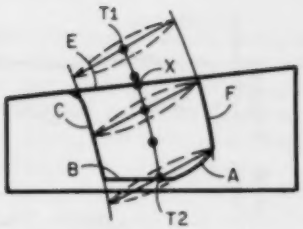

Figure 15.

bearing in this area. This is the sort of effect produced by an axial displacement of the pinion too large for the amount of profile mismatch provided.

Figure 16 shows the form in which TCA results are usually presented. The analysis has been performed for three separate running positions corresponding to toe, central, and heel contact as indicated by the three V/H values shown. Displacement curves and theoretical tooth bearings are shown for each running position.

This particular diagram shows practically perfect uniformity of motion transmission, since the scale used to plot the curves is very large; the value of 0.00002 radians indicated on the ordinate scale represents less than 0.0001 in. in peripheral motion of the gear. There is overlap in all cases, but little adjustability since a small amount of axial adjustment will change the slope of the curves and result in tip contact.

The tooth bearings are practically perfect; the paths of contact are straight and vertical, and the length and inclination of the contact marks are constant.

Mathematical Basis of TCA

A fundamental requirement of TCA is that the given tooth surfaces be generated in a completely arbitrary manner; that is, we must be prepared to analyze a pair of gears made with machine settings arrived at by some unknown procedure, or by trial-and-error. Similarly we must be able to analyze operation in relative running positions different from those specified on the drawings.

These requirements imply that we cannot make the assumption of uniform velocity transmission which so simplifies ordinary gear mesh analysis, and forces us to adopt a completely general procedure. As this procedure is described it will become evident that the

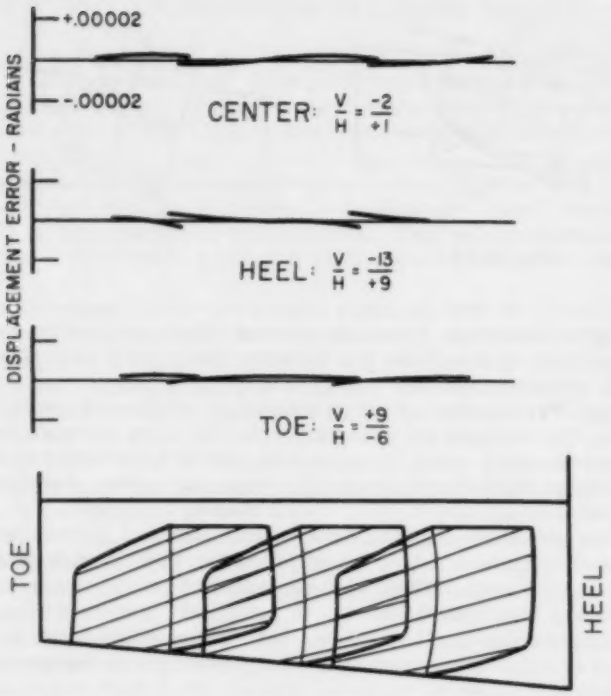

Figure 16.

calculation would be hopelessly long without the use of a high-speed electronic computer.

In general a point on a tooth surface can be specified by two parameters. In the case of generated tooth surfaces these parameters are taken to be the cradle angle q and an angle specifying rotational position around the cutter axis, θ; for FORMATE® or HELIXFORM® teeth convenient parameters are the distance s from the tip of the cutter blade to the specified point, and an angle α about the cutter axis.

If we assume a pair of values (q, θ) we can determine from the conditions of generation all we need to know about a specific point on the pinion tooth, including the direction of the tooth surface normal at that point. Similarly the choice of a pair of values (s, α) locates a point on the gear tooth with its normal. Since these points have been chosen arbitrarily, we have no assurance that they would ever

come into contact with the gears running in the specified relative position.

Nevertheless we can imagine the two gears to be physically moved into such a position that the two chosen points and their normals are coincident. Figure 17 indicates such an imaginary juxtaposition. Furthermore, we can imagine one of the gears to be rotated about the common surface normal, maintaining contact at the chosen points, until the angle between the shafts becomes the specified shaft angle Σ.

When this has been done the gear and pinion blanks are in a fixed relative position, and we can calculate the shaft offset E, and the axial positions x_p and x_G. These calculated values will not of course be the specified running positions, so we now proceed to change the assumed values of the three parameters θ, α, s until the values of E, x_p and x_G are correct, and thus obtain a point of contact. At this point of contact we can work out such details as the angular position of the gear and pinion, the instantaneous velocity ratio, and the curvature characteristics of the contacting tooth surface, that are required as part of the results of TCA.

Now by repeating the procedure with a different value of q we can obtain the sequence of contact points which makes up the path of contact.

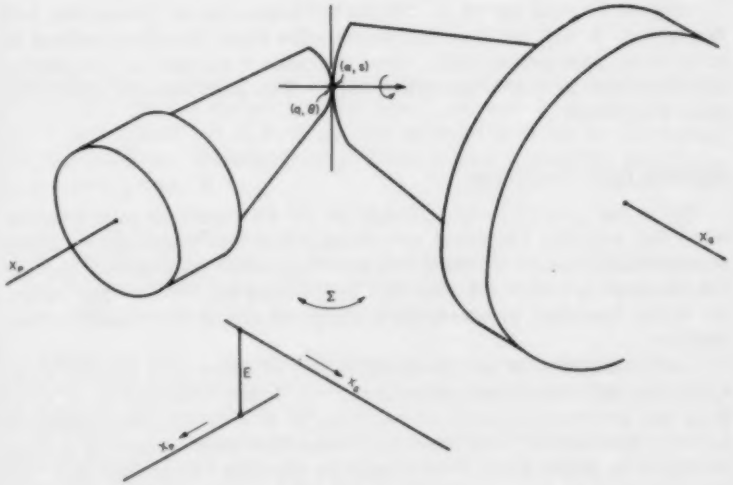

Figure 17.

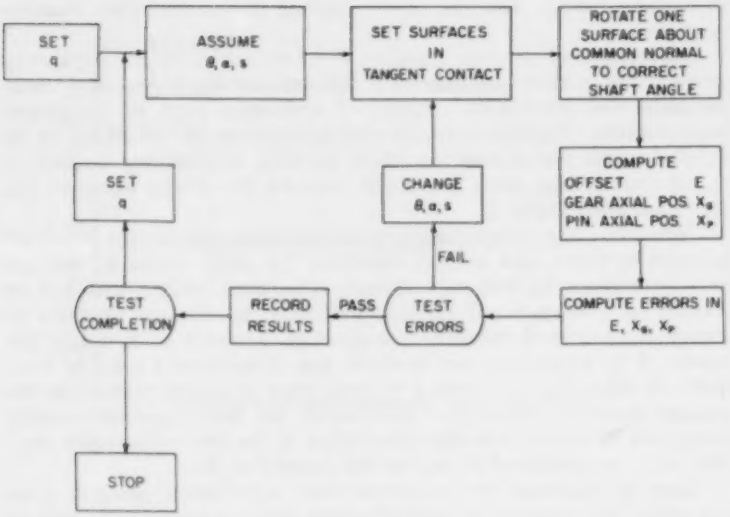

Figure 18.

Figure 18 will serve to clarify the sequence of operations just described. It will be seen that we require some iterative method to vary three parameters until three calculated errors, or residuals, become zero to some specified limit. The next section describes such a procedure.

Multiple Iteration Method

It is not particularly difficult to handle multiple interpolation when the relating functions are simple and short enough to make differentiation easy. In many engineering problems however this is not the case and we need a method which does not require any analysis of the functions involved, but merely the ability to calculate them rapidly.

Let us say that if we are given values of three parameters a, b, c, we can calculate three quantities, x, y, z which depend on a, b, c. It is not however possible to calculate a, b, c from given values of x, y, z. Nevertheless we must find somehow what values of a, b, c to choose to make $x = y = z = 0$, and we know as a practical fact that such a solution exists.

If we make a small change in a and determine its effect on x, y and z, we have obtained approximations of three partial derivatives

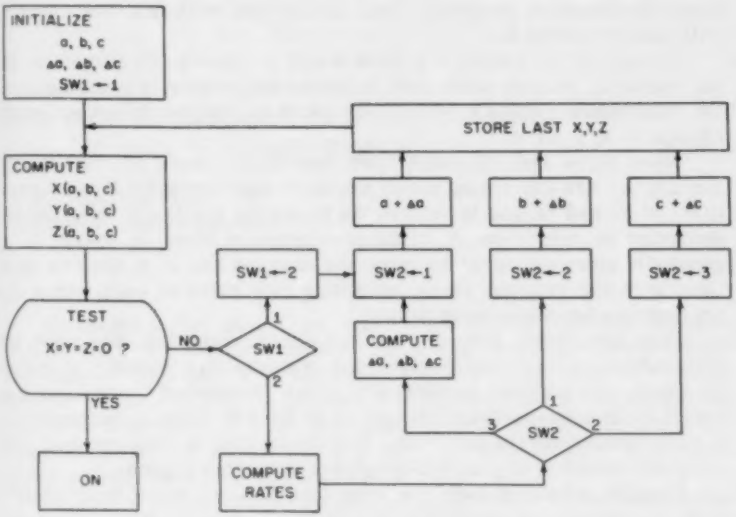

Figure 19.

$$\frac{\partial x}{\partial a}, \frac{\partial y}{\partial a}, \frac{\partial z}{\partial a}.$$

Similarly by stepping b and c small amounts we can complete the matrix of 9 partial derivatives or rates, and with these we can calculate new values for a, b, c merely by solving three simultaneous linear equations. Repeated application of this procedure will produce convergence, if

a) there is a unique answer
b) the starting values of the parameters are reasonable
c) high accuracy is maintained in computation, particularly in the solution of the linear equations.

Figure 19 is a computation flow-chart for one way of handling such an iterative procedure; not all necessary details are included, but only enough to indicate the plan.

We begin by initializing the starting values of a, b, c and specifying the small steps Δa, Δb, Δc to be used to get rates in the first pass. We also set switch 1 for the first pass.

The computational block calculates x, y and z, and the test block determines whether the errors are sufficiently small. If so, we exit

from the iteration program. Usually the test will fail and control will pass to switch 1.

Branch (1) of switch 1 resets itself to branch (2), proceeds to set switch 2, step a, store last answers and return to computation. On subsequent passes a new set of rates is figured following each change in a, b, or c.

When three sets of rates have been determined, new values of Δa, Δb, Δc are calculated which are first approximations to a solution. If we had reason to believe the functions are linear it would be desirable to substitute all of these changes at once; however it is generally more practical to apply the changes one at a time as was done with the original steps, obtaining new rates at each stage in preparation for subsequent passes.

This procedure, for one, two, or three variables, has been of tremendous value in our engineering computation; however it must of course be applied intelligently. One particularly troublesome condition is unsuspected discontinuity in the functional relationships; if such discontinuities exist they may be located in advance, and the program modified to prevent stepping across this region.

Multiple solutions have not been troublesome since their existence can usually be predicted, and sufficiently good starting values will force the solution we are after.

When the iteration does not converge, and the program has been carefully written to avoid round-off errors, we usually find that there is a physical meaning corresponding to the non-convergence. For example, in the TCA program, failure to converge indicates either

a) line contact instead of point contact, or
b) contact at or near the cusp of a generated surface.

Conclusion

This paper has developed a geometrical frame of reference for the study of hypoid gears; from this basis we have proceeded to a discussion of tooth contact in conjugate gear pairs with line contact, and then to the more important practical case of tooth contact in gear pairs so modified as to permit motion transmission under conditions of misalignment. As a necessary tool in the discussion, an iterative procedure has been described which has wide applicability in engineering work.

We hope that the material discussed here will have theoretical and practical value to both mathematicians and engineers.

3

Stress Concentration Caused by a Small Circular Hole in a Bent Plate

By Lajos Imre Nagy
General Motors Corporation

Consider a flat plate (see Fig. 1) bent at the ends by the moments (M). A concentric hole at the center of the plate will effect the stress distribution in the neighborhood of the hole by causing stress concentration. According to Saint-Venant's principle the effect of a small hole may be neglected at a distance of a few diameters from its edge. The points which are at such a distance from its edge can be regarded as being at infinity.

In order to solve the two-dimensional problem for finding the stresses at any point in the plate the equation of equilibrium, the compatibility equation,* and the boundary conditions must be satisfied.

By introducing the stress or Airy's Function ψ, the equations or equilibrium are automatically satisfied by taking the following expressions for stress components:

Two-dimensional cartesian coordinate system	Two-dimensional polar coordinates	
$\tau_{xx} = \frac{\partial^2 \psi}{\partial y^2}$	$\tau_{rr} = \frac{1}{r}\frac{\partial \psi}{\partial r} + \frac{1}{r^2}\frac{\partial^2 \psi}{\partial \theta^2}$	a,
$\tau_{yy} = \frac{\partial^2 \psi}{\partial x^2}$	$\tau_{\theta\theta} = \frac{\partial^2 \psi}{\partial r^2}$	b,
$\tau_{xy} = -\frac{\partial^2 \psi}{\partial x \partial y}$	$\tau_{r\theta} = -\frac{\partial}{\partial r}\left(\frac{1}{r}\frac{\partial \psi}{\partial \theta}\right)$	c,

(1)

By substituting the stress components into the compatibility equation, one may find that the stress function must satisfy the biharmonic equation:

*S. Timoshenko and J. N. Goodier, "Theory of Elasticity," page 230, equation 129, second edition, McGraw-Hill Book Company, Inc.

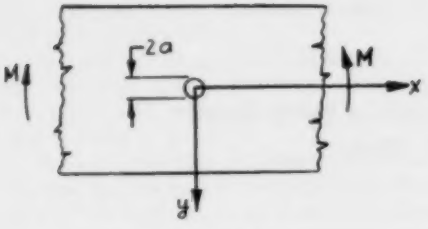

Figure 1

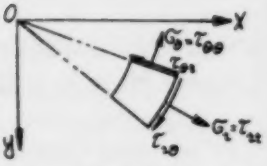

Figure 2

$$\frac{\partial^4 \psi}{\partial x^4} + 2\frac{\partial^4 \psi}{\partial x^2 y^2} + \frac{\partial^4 \psi}{\partial y^4} = 0 \quad - - - - - - - - - - - - \quad (2)$$

where $\frac{\partial^2}{\partial x^2} + \frac{\partial^2}{\partial y^2} = \nabla^2$ in cartesian coordinates

and $$\nabla^2 = \frac{\partial^2}{\partial r^2} + \frac{1}{r}\frac{\partial}{\partial r} + \frac{1}{r^2}\frac{\partial^2}{\partial \theta^2} \quad - - - - - - - - - - \quad (3)$$

in the polar coordinate system. ∇^2 is called the Laplace or Harmonic Operator. Thus equation (2) may also be written:

$$\nabla^2 \nabla^2 \psi = \nabla^4 \psi = 0$$

Assume a stress function such that $\psi = \psi_1 + \psi_2$, ψ_1 will be the stress function valid for the case if there is no hole present. ψ_2, will "correct the error committed" by not considering the hole.

The following boundary conditions have to be satisfied:

a) $\tau_{rr} = \tau_{xx} = -\frac{M y}{I}$ at $r = x \to \infty$ (well known equation for an intact bent plate)

b) $\tau_{rr} = 0$ at $r = a$ (no radial stress exists at the hole)

c) $\tau_{r\theta} = 0$ at $r = a$ (no tangential stress exists at the hole)

hence from Eq. (1a):

$$\frac{\partial \psi_1}{\partial y} = \int \tau_{xx}\, dy = -\int \frac{M y}{I}\, dy = -\frac{M y^2}{2 I} \text{ and } \psi_1 = -\int \frac{M y^2}{2 I}\, dy = -\frac{M y^3}{6 I}$$

since

$y = r \sin\theta$ and $\sin^3\theta = \frac{1}{4}[3\sin\theta - \sin(3\theta)]$, thus ψ_1 becomes

$$\psi_1 = -\frac{M r^3}{24 I}[3\sin\theta - \sin(3\theta)] \quad - - - - - - - - - \quad (4)$$

It may be shown that the stress function ψ_1 satisfies the biharmonic equation: $\nabla^4\psi_1 = 0$, thus the stress system shown below is compatible.

The stress components:

$$\left.\begin{aligned} \tau_{rr_1} &= \frac{1}{r}\frac{\partial\psi_1}{\partial r} + \frac{1}{r^2}\frac{\partial^2\psi_1}{\partial\theta^2} = -\frac{M r}{4 I}[\sin\theta + \sin(3\theta)] && \text{a,} \\ \tau_{\theta\theta_1} &= \frac{\partial^2\psi_1}{\partial r^2} = -\frac{M r}{4 I}[3\sin\theta - \sin(3\theta)] && \text{b,} \\ \tau_{r\theta_1} &= -\frac{\partial}{\partial r}\left(\frac{1}{r}\frac{\partial\psi_1}{\partial\theta}\right) = \frac{M r}{4 I}[\cos\theta - \cos(3\theta)] && \text{c,} \end{aligned}\right\} \quad (5)$$

It is convenient to assume ψ_2 in a similar manner as: (see Eq. 4)

$$\psi_2 = f_1(r)\sin\theta + f_2(r)\sin(3\theta)$$

According to Goursat's Theorem a Biharmonic Function (such as ψ_2) may always be expressed in the following form:

$$\psi_2 = F + r^2 G \quad \text{where} \quad \nabla^2 F = 0 \quad \text{and} \quad \nabla^2 G = 0$$

in other words F and G are harmonic functions. Since $f_1(r)\sin\theta$ also has to be a biharmonic function it can be assumed that it is composed of a harmonic term and the product of another harmonic term and r^2. If $f_1(r)\sin\theta$ were harmonic it would satisfy Laplace's equation.

Hence:

$$\frac{\partial^2}{\partial r^2}[f_1(r)\sin\theta] + \frac{1}{r}\frac{\partial}{\partial r}[f_1(r)\sin\theta] + \frac{1}{r^2}\frac{\partial^2}{\partial\theta^2}[f_1(r)\sin\theta] = 0$$

which may be rewritten as follows.

$$\sin\theta\frac{\partial^2}{\partial r^2}[f_1(r)] + \frac{\sin\theta}{r}\frac{\partial}{\partial r}[f_1(r)] - \frac{\sin\theta}{r^2}[f_1(r)] = 0$$

simplifying by $\sin\theta$

$$\frac{\partial^2}{\partial r^2} f_1(r) + \frac{1}{r}\frac{\partial}{\partial r} f_1(r) - \frac{1}{r^2} f_1(r) = 0 \quad - - - - - - - - (6)$$

The solution of Eq. 6 is the following:

$$f_1(r) = A' r + B r^{-1}$$

$f_1(r)$ is, however, biharmonic hence another term $(Cr + D r^{-1}) r^2$ has to be added. For $A' + D = A$ one obtains

$$f(r) = A r + B r^{-1} + C r^3 \quad - - - - - - - - - - (7)$$

The expression $f_2(r)$ may be found in a similar way. It can be shown that:

$$f_2(r) = E r^5 + F r^3 + G r^{-1} + H r^{-3} \quad - - - - - - - (8)$$

Thus $\psi_2 = f_1(r)\sin\theta + f_2(r)\sin(3\theta)$ is now a biharmonic expression and a stress system derived from it by means of equations 7, 8 and equation 5 will be compatible and in equilibrium.

The unknown constants: A, B, C, E, F, G and H may be determined by satisfying the boundary conditions.

$$\psi_2 = (A r + B r^{-1} + C r^3)\sin\theta + (E r^5 + F r^3 + G r^{-1} + H r^{-3})\sin(3\theta) \quad - - - (9)$$

Then:

$$\left.\begin{aligned} \tau_{rr_2} &= \frac{1}{r}\frac{\partial\psi_2}{\partial r} + \frac{1}{r^2}\frac{\partial^2\psi_2}{\partial\theta^2} \\ &= \left(\frac{A}{r} - \frac{B}{r^3} + 3Cr\right)\sin\theta + \left(5Er^3 + 3Fr - \frac{G}{r^3} - \frac{3H}{r^5}\right)\sin(3\theta) \\ &- \left(\frac{A}{r} + \frac{B}{r^3} + Cr\right)\sin\theta - \left(Er^3 + Fr + \frac{G}{r^3} + \frac{H}{r^5}\right)9\sin(3\theta) \end{aligned}\right\} \quad (10)$$

at $x \to \infty \quad \tau_{xx} = \tau_{rr}$

But $\tau_{xx} = -\frac{My}{I} = \tau_{rr_1}$ thus $\tau_{rr_2} = 0$ at $x = r \to \infty$

Therefore, the sum of the terms shown on the right hand side of Eq. 10 equal zero.

This is only possible if $C = E = F = 0$

Hence $$\tau_{rr_2} = -\frac{2B}{r^3}\sin\theta - \left(\frac{10G}{r^3} + \frac{12H}{r^5}\right)\sin(3\theta) \quad - - - (11)$$

Constant A vanishes in $\tau_{r\theta_2}$ and $\tau_{\theta\theta_2}$ also since

$$\tau_{r\theta_2} = -\frac{\partial}{\partial r}\left(\frac{1}{r}\frac{\partial\psi_2}{\partial\theta}\right) \quad \text{and} \quad \tau_{\theta\theta_2} = \frac{\partial^2\psi_2}{\partial r^2}$$

thus Eq. 9 becomes:

$$\psi_2 = Br^{-1}\sin\theta + (Gr^{-1} + Hr^{-3})\sin(3\theta) \quad - - - - - - (12)$$

From Eq. 12 (replacing ψ_1 by ψ_2 in Eq. 5)

$$\tau_{r\theta_2} = 2Br^{-3}\cos\theta + (2Gr^{-3} + 4Hr^{-5})\,3\cos(3\theta) \quad - - - (13)$$

and

$$\tau_{\theta\theta_2} = 2Br^{-3}\sin\theta + (2Gr^{-3} + 12Hr^{-5})\sin(3\theta) \quad - - - - (14)$$

According to boundary condition (b):

$$\tau_{rr} = \tau_{rr_1} + \tau_{rr_2} = 0 \quad \text{at} \quad r = a$$

Using equation (5a) and 11 and substituting "a" for "r" one may find that:

$$B = -\frac{Ma^4}{8I}$$

Boundary condition (c) states that:

$$\tau_{r\theta} = \tau_{r\theta_1} + \tau_{r\theta_2} = 0 \quad \text{at} \quad r = a$$

It can be shown that this leads to the following values:

$$G = -\frac{Ma^4}{8I} \quad \text{and} \quad H = \frac{Ma^6}{12I}$$

Thus from Eq. (4) and (12)

$$\psi = \psi_1 + \psi_2 = -\frac{M}{8rI}(r^4 + a^4)\sin\theta + \frac{Mr^3}{24I}\left(2\frac{a^6}{r^6} - 3\frac{a^4}{r^4} + 1\right)\sin(3\theta)$$

Also:

$$\left.\begin{aligned}
\tau_{rr} &= \tau_{rr_1} + \tau_{rr_2} = \frac{Mr}{4I}\left(\frac{a^4}{r^4} - 1\right)\sin\theta + \frac{Mr}{4I}\left(-4\frac{a^6}{r^6} + \frac{5a^4}{r^4} - 1\right)\sin(3\theta) \\
\tau_{r\theta} &= \tau_{r\theta_1} + \tau_{r\theta_2} = \frac{Mr}{4I}\left(1 - \frac{a^4}{r^4}\right)\cos\theta + \frac{Mr}{4I}\left(4\frac{a^6}{r^6} - 3\frac{a^4}{r^4} - 1\right)\cos(3\theta) \\
\tau_{\theta\theta} &= \tau_{\theta\theta_1} + \tau_{\theta\theta_2} = -\frac{Mr}{4I}\left(\frac{a^4}{r^4} + 3\right)\sin\theta + \frac{Mr}{4I}\left(4\frac{a^6}{r^6} - \frac{a^4}{r^4} + 1\right)\sin(3\theta)
\end{aligned}\right\} \quad (15)$$

Equations (15) determine the three stress components at any point of the plane given by r and θ. These stresses are compatible, while satisfying the equilibrium, and boundary conditions. The maximum occurs at the circumference of the hole. (r = a)

Here $\tau_{rr} = \tau_{r\theta} = 0$

and $$(\tau_{\theta\theta})_{r=a} = -\frac{Ma}{I}\left[\sin\theta - \sin(3\theta)\right] - - - - - - - - (16)$$

It is known that:

$$\sin(3\theta) = 3\sin\theta - 4\sin^3\theta$$

Therefore:

$$(\tau_{\theta\theta})_{r=a} = -\frac{Ma}{I}\,2\sin\theta(2\sin^2\theta - 1) - - - - - - - - (17)$$

$$(\tau_{\theta\theta})_{r=a} = 0 \qquad \text{for} \qquad \theta = n\pi$$

or $$\theta = \frac{\pi}{4}(2n + 1) \qquad \text{where} \qquad n = 0,1,2,3, \cdots$$

In order to find the maximum value of $(\tau_{\theta\theta})_{r=a}$ differentiate it with respect to θ and set it equal to zero.

$$\frac{d\tau_{\theta\theta}}{d\theta} = \frac{Ma}{I}(12\sin^2\theta\cos\theta - 2\cos\theta) = 0$$

Thus

$$12\sin^2\theta = 2 \qquad \text{Hence} \qquad \theta = n\pi \pm 24.15^0$$

or if $\cos\theta = 0$ so $\sin\theta = \pm 1$ and

$$\theta = \frac{\pi}{2}(2n + 1)$$

where again $n = 0,1,2,3, \cdots$

The latter value yields a maximum stress of

$$(\tau_{\theta\theta})_{\substack{\max. \\ r=a}} = \pm 2\frac{M a}{I}$$

Hence the maximum stress is twice the stress calculated by means of the elementary theory. In other words the factor of stress concentration is 2.

It is interesting to note that $(\tau\theta\theta)_{r=a}$ reaches the maximum value at $\theta = \frac{\pi}{2}(2n + 1)$ but it is not necessarily the maximum stress of the whole system.

Denoting $\eta = \frac{a}{r}$ and $\theta = \frac{\pi}{2}(2n + 1)$ in Eq. (15) one may obtain the following:

$$\tau_{\theta\theta} = \pm \frac{M r}{I}(1 + \eta^6) \qquad \text{when} \qquad \eta \leq 1$$

Denote $K = 1 + \eta^6 = 1 + \frac{a^6}{r^6}$

Thus $$\tau_{\theta\theta} = \pm K\frac{M r}{I} \tag{18}$$

In order to draw the stress diagram, let $a = 1$ and r vary from 1 to 7. From Eq. (18) it is easy to establish a chart and the stress diagram shown below. (See Fig. 3)

a = 1	
r	K·r
1	2.00000
2	2.03125
3	3.00412
4	4.00098
5	5.00032
6	6.00013
7	7.00006

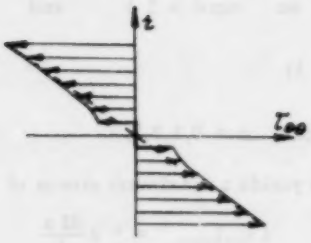

Figure 3

The dotted line represents the stress distribution without the hole, and the solid line indicates the present one.

Thus the effect of the hole will be negligible at a few diameters distance away.

The negative sign denotes the compressive stress and the positive sign denotes the tensile stress.

LITERATURE

C. T. Wang, *Applied Elasticity*, McGraw-Hill Book Co., Inc.

S. Timoshenko and S. Woinowsky-Krieger, *Theory of Plates and Shells*, McGraw-Hill Book Co., Inc.

E. G. Coker and L. N. G. Filon, *Photo-Elasticity*, Cambridge University Press, 1931.

M. M. Frocht, *Photoelasticity (2 Vols.)*, John Wiley &Sons, Inc.

4

A Graph for Determining CSP-5 Continuous Sampling Plans

By John S. White
Mathematics Group
General Motors Research Laboratories

Two new single level continuous sampling plans were recently proposed by Derman, Johns, and Lieberman (1). These plans, called CSP-4 and CSP-5, are essentially modifications of Dodge's original continuous sampling plan CSP-1 (2). The new plans are best described by setting forth their procedures as compared with that for CSP-1. The procedures for CSP-1, CSP-4, and CSP-5 are as follows.

(a) At the outset, inspect 100% of the units consecutively as produced and continue such inspection until i units in succession are found clear of defects.

(b) When i units in succession are found clear of defects, discontinue 100% inspection, and inspect only a fraction $f = 1/k$ of the units,

(b-1) selecting individual sample units one at a time from the flow of product, in such a manner as to assure an unbiased sample.

(b-4,5) choosing the unit to be inspected at random from a segment of size k.

(c) If a sample unit is found defective,

(c-1) revert immediately to 100% inspection of succeeding units and continue until again i units in succession are found clear of defects, as in paragraph (a).

(c-4) revert immediately to 100% inspection, eliminating from the production process the remaining (k-1) units in the segment, and commencing 100% inspection with the next unit following the eliminated segment. Continue 100% inspection until again i units in succession are found clear of defects, as in paragraph (a).

Table 1. AOQL(In Percent), Clearance Number (I), and Sampling Frequency (F) for CSP-5

I	F=1/2	F=1/3	F=1/4	F=1/5	F=1/7	F=1/10	F=1/15	F=1/25	F=1/50	F=1/100	F=1/200	I
2	4.4006	10.460	18.718	14.308	16.436	18.361	20.096	21.795	23.223	24.062	24.516	2
3	3.866	9.825	10.661	12.150	14.228	16.197	18.155	20.119	22.079	23.345	24.101	3
4	3.466	7.922	7.311	7.132	10.803	12.844	14.959	16.324	18.457	20.738	22.371	4
5	3.192	7.311	7.098	7.093	7.093	12.033	13.951	15.911	18.013	19.341	21.250	5
6	3.096	5.583	7.098	7.370	8.916	10.310	13.908	15.537	16.045	20.087	22.029	6
7	3.108	4.989	6.332	7.370	8.916	10.310	12.267	14.220	16.031	18.952	20.481	7
8	2.797	4.508	5.738	6.695	8.131	9.330	11.222	13.345	15.735	17.880	19.459	8
9	2.643	4.111	5.244	6.132	7.469	8.876	10.445	12.346	15.735	16.972	19.042	9
10	2.531	3.778	4.830	5.654	6.905	8.229	9.714	11.533	13.658	16.972	17.802	10
11	2.151	3.494	4.474	5.245	6.419	7.667	9.076	10.816	13.062	15.139	17.802	11
12	1.997	3.250	4.167	4.891	5.996	7.175	8.514	10.176	12.345	14.370	16.211	12
13	1.864	3.038	3.900	4.581	5.624	6.742	8.016	9.606	11.698	13.671	15.492	13
14	1.747	2.851	3.664	4.308	5.296	6.358	7.572	9.095	11.112	13.031	14.819	14
15	1.644	2.686	3.455	4.065	5.003	6.014	7.174	8.634	10.579	12.444	14.196	15
16	1.552	2.539	3.269	3.848	4.741	5.705	6.815	8.216	10.093	11.904	13.618	16
17	1.471	2.408	3.101	3.653	4.505	5.427	6.489	7.857	9.648	11.407	13.082	17
18	1.397	2.289	2.950	3.477	4.291	5.173	6.193	7.490	9.240	10.944	12.583	18
19	1.330	2.181	2.813	3.317	4.096	4.943	5.923	7.172	8.864	10.522	12.119	19
20	1.270	2.083	2.688	3.171	3.918	4.732	5.675	6.879	8.517	10.128	11.686	20
21	1.214	1.994	2.574	3.037	3.755	4.538	5.447	6.610	8.195	9.761	11.281	21
22	1.164	1.912	2.469	2.914	3.605	4.359	5.236	6.360	7.897	9.419	10.902	22
23	1.117	1.836	2.372	2.801	3.467	4.194	5.041	6.128	7.619	9.100	10.547	23
24	1.074	1.766	2.282	2.696	3.338	4.040	4.859	5.913	7.359	8.801	10.214	24
25	1.034	1.701	2.199	2.598	3.219	3.898	4.691	5.712	7.117	8.520	9.900	25
26	0.997	1.641	2.122	2.508	3.108	3.765	4.533	5.524	6.889	8.257	9.605	26
27	0.963	1.585	2.050	2.423	3.004	3.641	4.386	5.348	6.676	8.009	9.326	27
28	0.930	1.532	1.983	2.344	2.907	3.525	4.248	5.182	6.475	7.775	9.062	28
29	0.900	1.483	1.920	2.270	2.816	3.416	4.118	5.027	6.286	7.555	8.815	29
30	0.872	1.437	1.861	2.201	2.731	3.313	3.996	4.881	6.108	7.346	8.577	30
31	0.846	1.393	1.804	2.135	2.651	3.217	3.881	4.742	5.939	7.148	8.353	31
32	0.821	1.353	1.753	2.074	2.575	3.126	3.772	4.612	5.779	6.961	8.140	32
33	0.797	1.315	1.703	2.016	2.503	3.039	3.670	4.488	5.628	6.785	7.937	33
34	0.775	1.279	1.657	1.961	2.435	2.958	3.572	4.371	5.486	6.618	7.744	34
35	0.754	1.244	1.612	1.908	2.371	2.881	3.480	4.260	5.353	6.459	7.560	35
36	0.734	1.212	1.570	1.859	2.310	2.807	3.393	4.154	5.218	6.308	7.385	36
37	0.715	1.181	1.531	1.812	2.253	2.738	3.309	4.053	5.094	6.163	7.217	37
38	0.697	1.152	1.493	1.768	2.197	2.671	3.230	3.957	4.976	6.024	7.057	38
39	0.680	1.124	1.457	1.725	2.145	2.608	3.154	3.866	4.863	5.888	6.904	39
40	0.664	1.097	1.422	1.685	2.095	2.548	3.082	3.779	4.755	5.758	6.759	40
41	0.649	1.072	1.390	1.646	2.047	2.490	3.013	3.695	4.652	5.630	6.616	41
42	0.634	1.047	1.358	1.609	2.002	2.435	2.947	3.615	4.553	5.512	6.481	42
43	0.620	1.024	1.329	1.574	1.958	2.383	2.884	3.539	4.458	5.400	6.351	43
44	0.606	1.002	1.300	1.540	1.917	2.332	2.823	3.465	4.367	5.292	6.226	44
45	0.593	0.981	1.273	1.508	1.877	2.284	2.765	3.395	4.280	5.188	6.107	45
46	0.581	0.961	1.246	1.477	1.838	2.238	2.710	3.327	4.196	5.088	5.991	46
47	0.569	0.941	1.221	1.447	1.801	2.193	2.656	3.262	4.115	4.992	5.880	47
48	0.558	0.922	1.197	1.419	1.766	2.150	2.605	3.200	4.038	4.899	5.773	48
49	0.547	0.904	1.174	1.391	1.732	2.109	2.555	3.140	3.963	4.810	5.669	49
50	0.536	0.887	1.151	1.365	1.699	2.070	2.508	3.082	3.891	4.724	5.570	50

(c-5) screen the remaining (k-1) items in the segment. Upon completion of this screening, commence 100% inspection with the next unit produced. Continue 100% inspection until again i units in succession, not including the (k-1) screened items, are found clear of defects, as in paragraph (a).

(d) Correct or replace with good units all defective units found.

Each of the plans CSP-1, CSP-4, and CSP-5 follows the above procedure except that each follows the subsections of paragraphs (b) and (c) which correspond to the plan number.

If the production process is "in control" with a defect rate of p(q = 1 - p) then the respective AOQ functions are

$$\text{AOQ(CSP-1)} = \frac{(k-1)pq^i}{1 + (k-1)q^i}$$

$$\text{AOQ(CSP-4)} = \frac{(k-1)pq^{i+1}}{1 + (k-1)q^{i+1}}$$

$$\text{AOQ(CSP-5)} = \frac{(k-1)pq^{i+1}}{1 + (k-1)q^i}$$

From the form of the AOQ functions we see that the AOQL of a CSP-4 plan with a given f = 1/k and i is the same as that for a CSP-1 plan with the same f but with clearance number i + 1. Thus specific CSP-4 plans may easily be obtained from available tables and graphs (2,3,4) for CSP-1.

Although the AOQ function for CSP-5 differs from that of CSP-1 by only a factor of q, there appears to be no simple analytic method of obtaining the CSP-5 AOQL from that of CSP-1. The AOQL for CSP-5 plans for the set of sampling fractions used in H-107 was computed and the results appear in Figure 1. For $i \leq 50$, the exact AOQL's for certain f values are given in Table 1.

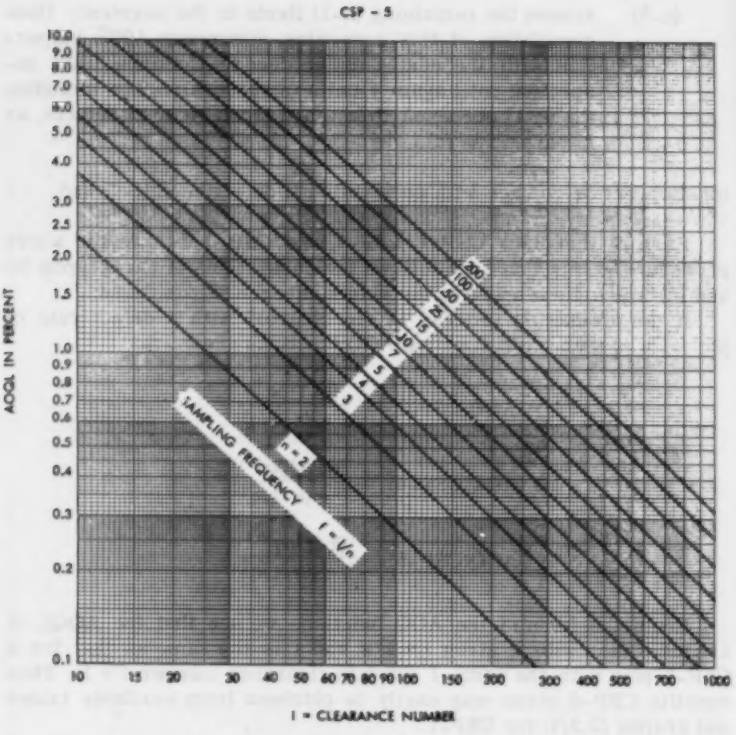

Figure 1

REFERENCES

(1) C. Derman, M. V. Johns, and G. J. Lieberman, "Continuous Sampling Procedures Without Control," Annals of Mathematical Statistics, Vol. 30 (1959), 1175-1191.

(2) H. F. Dodge, "A Sampling Inspection Plan for Continuous Production," Annals of Mathematical Statistics, Vol. 14 (1943), 264-279.

(3) "H-107: Single-Level Continuous Sampling Procedures and Tables for Inspection by Attributes," U. S. Government Printing Office, Washington, D. C. (1959).

(4) J. S. White, "A New Graph for Determining CSP-1 Sampling Plans," Industrial Quality Control (Accepted for publication).

5

Introduction to Nonlinear Tchebycheff Approximation

By John R. Rice

1. THE PROBLEM.

The *linear approximation problem* is as follows: Given a function f(x) and a set of n functions $\{\varphi_i(x)\}$, find the parameters (or coefficients) a of the approximating functions

$$(1.1) \qquad L(A,x) = \sum_{i=1}^{n} a_i \varphi_i(x) \qquad A = (a_1, a_2, \ldots, a_n)$$

which makes L(A,x) as "close" to f(x) as possible. There are a variety* of ways to measure how "close" L(A,x) is to f(x). In this article we consider the Tchebycheff (or uniform) measure. Thus L(A,x) is required to minimize

$$(1.2) \qquad \max_{x \in [0,1]} |L(A,x) - f(x)|$$

The specific interval [0,1] of approximation is used throughout this article, though the discussion is valid for any interval.

The nonlinear approximation problem is identical with the linear approximation problem except that the approximating function F(A,x) no longer depends linearly on the parameters. The approximating function F(A,x) is assumed to depend continuously on the parameters. The problem is formally stated as

*The most common way is to minimize

$$\int [L(A,x) - f(x)]^2 \, dx$$

For linear approximation this least squares measure has the advantage that the parameters may be computed directly. However, there are no direct methods for nonlinear least squares approximations and there is some evidence that nonlinear Tchebycheff approximations may be computed with less difficulty for certain approximating functions.

NONLINEAR TCHEBYCHEFF PROBLEM: *Given f(x) continuous on [0,1] determine parameters A* so that*

$$\max_{x \in [0,1]} |F(A^*,x) - f(x)| \leq \max_{x \in [0,1]} |F(A,x) - f(x)|$$

for all parameters A.

This article gives an informal account of some recent developments in the theory associated with this problem. The method of presentation is to first consider very simple examples in some detail. An "intuitive feel" for the problem is thus obtained. The general results are then obtained from an abstraction of the essential elements of these examples. No formal proofs are given.

There are three principal questions associated with this problem. They are

1. Does a best approximation exist?
2. If so, is it unique?
3. What properties are characteristic of a best approximation?

The first two questions are, of course, of basic interest, but the answer to the third question is the most important from the practical viewpoint. For it is these properties which distinguish the best approximations from other approximations, and the methods of computation are based on them.

2. APPROXIMATION BY POLYNOMIALS.

First let us consider the simplest possible case, namely when F(A,x) depends on one parameter a and

$$F(A,x) \equiv a.$$

For any approximation a_1 to f(x), consider the *error curve* $f(x) - a_1$ in Figure 1. The maximum error occurs at x_1. It is easy to see that if we increase a slightly (say to the dotted line), we can decrease $\max |f(x) - a|$. Indeed we can increase a until the error at x_2 becomes as large as the error at x_1. At this point we cannot improve the approximation by varying a. If we decrease the error at x_1 we increase it at x_2 and vice versa. Thus in this simple case we can get a formula for the best Tchebycheff approximation,

$$a^* = \frac{1}{2}\left[\max_{x \in [0,1]} f(x) - \min_{x \in [0,1]} f(x)\right] \tag{2.1}$$

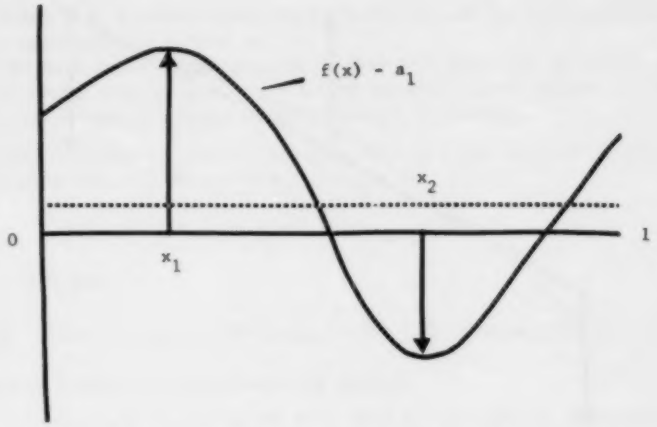

Figure 1. Approximation by a Constant

We now consider the next simplest problem, namely approximation by

$$F(A,x) = a + b\,x \tag{2.2}$$

We again examine our error curve in Figures 2a, 2b, which represent the same situation.

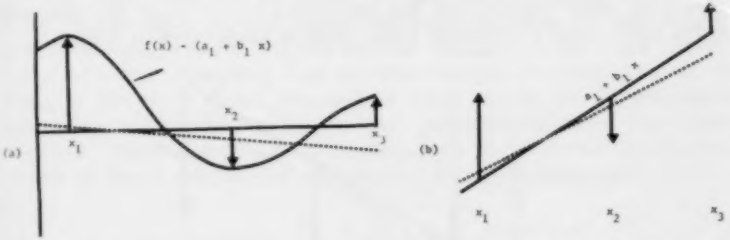

Figure 2. The Error Curves of a Trial Approximation to f(x).

The largest error occurs at x_1. Clearly we can adjust the constant a_1 so as to decrease the error at x_1 at the expense of increasing it at x_2. However, we can actually do more. We can reduce the error at *both* x_1 and x_2 by adjusting *both* of the parameters a and b. Such an adjustment is shown by the dotted line. This process may be

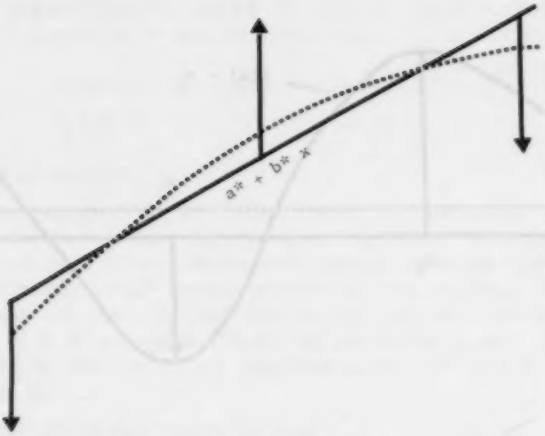

Figure 3. In order to reduce the error at three points the approximation must cross a* + b* x twice.

continued until the error at x_3 becomes as large as the maximum error. As long as the three errors are not the same size, the largest two may be reduced by varying a and b. Once the three errors are equal we cannot improve the approximation. This is illustrated in Figure 3. Since the errors are all equal a better approximation than a* + b* x must cross a* + b* x twice. This implies that the better approximation is curved, which is not possible for a line. Note that it is not sufficient for the maximum error to be assumed three times, but the maximum error must be assumed three times with *alternating sign*. This is illustrated in Figure 4.

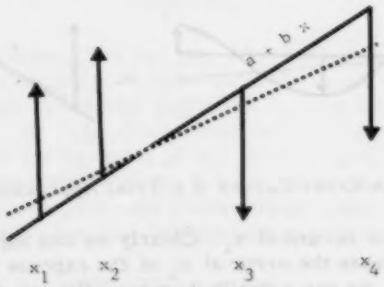

Figure 4. The maximum error is assumed 4 times, but a + b x is not a best approximation.

In Figure 4 if one decreases the error at x_1 and x_3, it is automatically decreased at x_2 and x_4.

We have come to the conclusion that $a^* + b^* x$ can be a best approximation only if the error curve appears as in Figure 3. We give this situation a name in the following definition:

DEFINITION 1. *The error curve $F(A,x) - f(x)$ is said to alternate n times if these are $n + 1$ points*

$$0 \leq x_1 < x_2 < \ldots < x_{n+1} \leq 1$$

such that

$$(2.3) \quad F(A,x_i) - f(x_i) = -[F(A,x_{i+1}) - f(x_{i+1})] = \pm \max |F(a,x) - f(x)|$$

We may restate this conclusion by saying:

A necessary condition for $a^* + b^* x$ to be a best approximation to $f(x)$ is that $a^* + b^* x - f(x)$ alternates at least twice.

We may also conclude from Figure 3 that

A sufficient condition for $a^* + b^* x$ to be a best approximation to $f(x)$ is that $a^* + b^* x - f(x)$ alternates at least twice.

In these two statements we have answered the third question associated with the approximation problem for (2.2). Best approximations to $f(x)$ are characterized as exactly those approximations $a^* + b^* x$ such that $a^* + b^* x - f(x)$ alternates at least twice.

There is a slightly different way to look at approximation by $a + b x$. There are two parameters which may be varied in $a + b x$. They may be used to "push down" the error curve at any two points. When one "pushs down" the two largest "humps" on the error curve, there is a corresponding rise in other humps. As soon as a third hump of the error curve becomes as large as the two largest ones (including alternation of sign) the best approximation has been reached. The fact that the error curve may be "adjusted" at *any* two points is due to the fact that the parameters are independent, i.e.

$$(2.4) \quad \begin{vmatrix} 1 & x_1 \\ 1 & x_2 \end{vmatrix} \neq 0$$

for $x_1 \neq x_2$.

We may briefly examine this line of reasoning for approximation by

$$(2.5) \quad F(A,x) = a + b x + c x^2$$

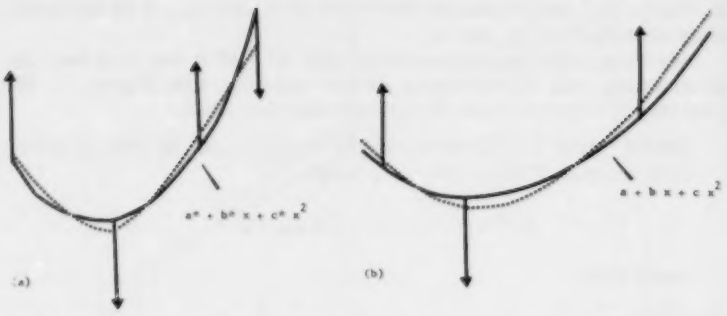

Figure 5. Alternation 2 and 3 times for a quadratic approximation.

The situation of alternation 3 times is illustrated in Figure 5. In Figure 5b $a + bx + cx^2 - f(x)$ alternates only twice and we can find a parabola (i.e., a function of the form (2.5)) which decreases the error at each of the three points where the maximum error is attained. Such a parabola is shown by the dotted line. In order to reduce the maximum error in Figure 5a an improved approximation (shown dotted) must intersect $a^* + b^*x + c^*x^2$ at least 3 times. This is impossible for parabolas. We have then arrived at the same type of characterization for quadratic approximation as for approximation by $a + bx$.

We now turn to the most general linear approximating function (1.1). There were two properties of polynomials that were used to obtain the characterization of best approximation by alternation. The first was the ability to "push down" the error curve at any n points (for n parameters). For the approximating function $L(A,x)$ we may obtain this ability by assuming

$$(2.5) \qquad \begin{vmatrix} \varphi_1(x_1) & \varphi_1(x_2) & \cdots & \varphi_1(x_n) \\ \varphi_2(x_1) & \varphi_2(x_2) & \cdots & \varphi_2(x_n) \\ \cdot & \cdot & \cdots & \cdot \\ \varphi_n(x_1) & \varphi_n(x_2) & \cdots & \varphi_n(x_n) \end{vmatrix} \neq 0$$

for any set of n distinct points $\{x_i\}$. This condition then implies that alternation at least n times is necessary for best approximation. The second property of polynomials used is the fact that two distinct polynomials of nth degree can intersect at most n times.* This

*This is more commonly stated by saying that a polynomial of nth degree has at most n zeros.

property for L(A,x) also follows from condition (2.5). Thus if we assume the set of functions $\{\varphi_i(x)\}$ satisfy (2.5) we find that best approximations are characterized by alternation of the error curve at least n times. A set of functions satisfying (2.5) is called a *Tchebycheff set* [1], [2].

We now turn to the first two questions. It is always true that there is a sequence $\{A_i \mid i = 1, 2, \ldots\}$ of parameters so that

$$\lim_{i \to \infty} \max |L(A_i,x) - f(x)| = \inf_{A} \max |L(A_i,x) - f(x)|$$

We need only to know that this sequence possesses a limit. Due to the linear dependence of L(A,x) on A, the set $\{L(A_i,x)\}$ is an equicontinuous set of functions. Thus the sequence $\{L(A_i,x) \mid i = 1, 2, \ldots\}$ contains a convergent subsequence and the limit of this subsequence exists and is a best approximation L(A*,x) to f(x).

The uniqueness of the best approximation by L(A,x) follows from the fact that $L(A^*_1,x) - L(A^*_2,x)$ can have at most n - 1 zeros. This is a consequence of (2.5).

We can now state the following theorem which gives the principal points of linear Tchebycheff approximation. [1], [2], [11].

THEOREM 1 - *Let f(x) and $\varphi_i(x)$ be continuous on [0,1]. If $\{\varphi_i(x)\}$ satisfies (2.5) then we have*

A. *a best approximation L(A*,x) to f(x) exists*

B. L(A*,x) *is unique*

C. L(A*,x) *is the best approximation to f(x) if and only if* L(A*,x) - f(x) *alternates at least n times on [0,1]*

Theorem 1(A) follows from the fact that L(A,x) is linear in A. Theorem 1(B) follows from the fact that $L(A_1,x) - L(A_2,x)$ may have at most n - 1 zeros; the if portion of Theorem 1(C) also follows from this. The only if portion of Theorem 1(C) follows from the fact that we may "push down" the error curve at any n points. Actually, this theorem follows from only two things, linearity and (2.5), however when we consider nonlinear approximation condition (2.5) will disappear and be replaced by conditions similar to those given here which are (in the linear case) consequences of (2.5).*

*Motzkin [3] and Tornheim [10] have defined unisolvent families and n-parameter families, respectively where properties equivalent to the "n-1 zero properties" and "push down" property are abstractly assumed. For any nonlinear approximating function with these properties Theorem 1ABC is valid. The elementary nonlinear approximating functions do not have these properties.

3. APPROXIMATION BY $AB^x + C$ ON $[0,1]$.

We now consider a simple example of a nonlinear approximating function in order to see what one may expect. We consider approximation as follows:

$$ab^x + c \sim f(x) \qquad x \in [0,1] \tag{3.1}$$

The first question that we need to consider is: do best approximations exist for all continuous functions? If we have a sequence $\{a_i b_i^x + c_i\}$ so that

$$\lim_{i \to \infty} \max |a_i b_i^x + c_i - f(x)| = \inf_{a,b,c} \max |ab^x + c - f(x)|, \tag{3.2}$$

this sequence must certainly remain bounded. Some possibilities for behavior of this sequence are shown in Figure 6.

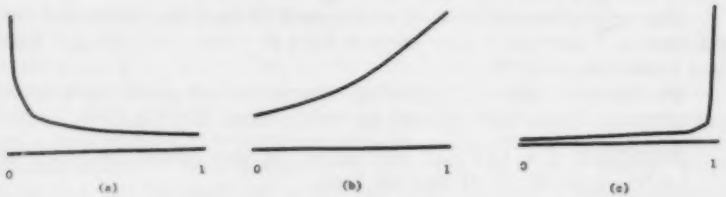

Figure 6. Some exponentials.

The limits for case (a) may be

$$D(x) = \begin{cases} a + c & x = 0 \\ c & 0 < x \le 1 \end{cases} \tag{3.3}$$

However, this approximation is no better than the constant c. This is a manifestation of the fact that one cannot improve an approximation by changing its value at only one point. Hence we identify all "curves" (3.3) with the constant c. The same approach applies for Figure 6c. In Figure 6b, nothing much happens; the exponentials just settle down to another exponential *OR* to a line. A little thought shows that we cannot find a best approximation to a straight line. The maximum error may be made arbitrarily small, but $a b^x + c$ is never actually a line. We may avoid this embarrassing situation by simply extending the definition of our approximating functions to

$$E(A,x) = \begin{cases} a b^x + c & b \neq 1 \\ c + d x & b = 1 \text{ or } a = 0 \end{cases} \tag{3.4}$$

For L(A,x) we are able to "push down" the error curve at any n points (here to number of parameters is 3, so n = 3). Let us examine E(A,x) for a similar property. See Figure 7.

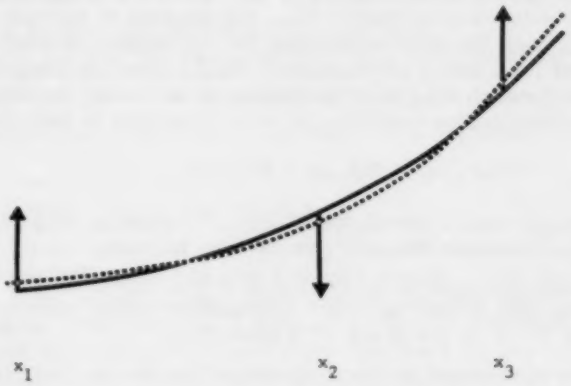

Figure 7. Improvement of the approximation at 3 points.

To approve the approximation at x_1, x_2 and x_3 one increases c slightly, decreases a and increases b. One can do the same thing for a straight line. Thus it is seen that if the error curve alternates only twice then one can improve the approximation. However, there is one exception and that occurs where b = 1, d = 0 (or alternatively a = 0).

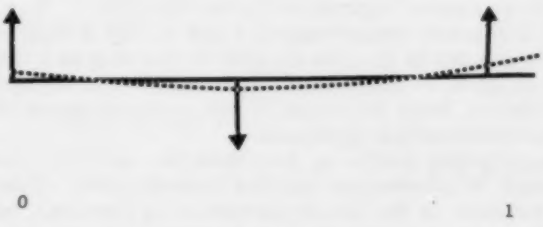

Figure 8. The degenerate case of a b^x + c = constant.

There is no possibility for a function E(A,x) to behave as the dotted line in Figure 8, for every E(A,x) is monotonic. Hence, we arrive at the following conclusion:

If $b \neq 1$, $d \neq 0$ (or $a \neq 0$) then 3 alternations of the error curve are necessary for $E(A^*,x)$ to be a best approximation to $f(x)$. If $b = 1$, $d = 0$ (or $a = 0$) then only 2 alternations are necessary.

Thus the number of alternatives necessary for a heat approximation depends on the best approximation. The question of interest at this point is: does the same result hold for the number of alternations *sufficient* for a best approximation? Recall from the linear theory that this question relates to the number of zeros that the difference of two approximating functions can have. It is easy to show that

$$E(A_1,x) - E(A_2,x) \tag{3.5}$$

can have at most 2 zeros, *and* if $E(A_1,x)$ = constant then (3.5) can only have one zero. Therefore we have the following.

CHARACTERIZATION. *$E(A^*,x)$ is a best approximation to $f(x)$ if and only if $E(A^*,x) - f(x)$ alternates k times where $k = 2$ if $b = 1$, $d = 0$ (or $a = 0$) and $k = 3$ otherwise.*

The uniqueness of the best approximation follows from the discussion of the number of zeros of (3.5) in the same way as for linear approximating functions.

It should be noted here that a condition analogous to (2.5) is not present. The questions of the number of zeros of (3.5) and the ability to "push down" the error curve have become separated. The question of the existence of best approximations has remained a separate problem.

4. ABSTRACTION TO VARISOLVENT FUNCTIONS.

In this section we extend the theory indicated by the example of $a\,b^x + c$ to an abstract approximating function $F(A,x)$. It is assumed that $F(A,x)$ depends continuously on A and x. The domain of parameters A is denoted by P. The set P is viewed only as a set to index the various functions represented by $F(A,x)$. It is sometimes possible (but often not easy) to identify P with a simple subset of Euclidean space of appropriate dimension.

In the preceding section we have seen that there is a characteristic number of alternations for best approximation. This number is not a constant, as for linear approximating functions, but rather is a function of the particular best approximation, or equivalently, of the parameters A. This idea can be abstracted as follows:

DEFINITION 2. *$F(A,x)$ is a varisolvent function if there exists a degree $m(A)$ defined on P such that $F(A^*,x)$ is a best approximation to $f(x)$ if and only if $F(A^*,x) - f(x)$ alternates $m(A^*)$ times.*

This is not the usual or original definition of a varisolvent function. The original definition [6] says F is varisolvent if F has the following properties:

PROPERTY Z. $F(A,x) - F(A^*,x)$ *has at most* $m(A^*) - 1$ *zeros.*

PROPERTY OF SOLVENCE. *given* $\{x_j \mid j = 1, 2, \ldots, m(A^*)\}$ *and* $\epsilon > 0$ *then there exists a* $\delta(A^*, \epsilon, x_j) > 0$ *such that*

$$|F(A^*, x_j) - Y_j| < \epsilon$$

implies that there exists a solution A to the equations

$$F(A, x_j) = Y_j \qquad j = 1, 2, \ldots, m(A^*)$$

with max $|F(A,x) - F(A^*,x)| < \epsilon$.

Property Z is the property of linear approximating functions used to establish the sufficiency of $m(A^*)$ alternations for best approximation. This property also implies that best approximations are unique. The Property of Solvence is an $\epsilon - \delta$ statement of what is meant by being able to "push down" the error curve at any $m(A^*)$ points. It is one of the deeper results [5] of approximation theory that these two definitions are equivalent.*

For varisolvent approximating functions the characterization and uniqueness of best approximations are intimately connected by Property Z. The question of the existence of best approximations is completely separated.

5. EXAMPLES.

In this section a few known and conjectured examples of varisolvent functions are given.

1. *Rational Function* [1].

$$R(A,x) = s(x) \frac{\sum_{i=0}^{n} a_i x^i}{\sum_{j=0}^{m} b_j x^j}, \quad \frac{s(x) > 0, \; x \in [0,1]}{\sum_{j=0}^{m} b_j x^j > 0, \; x \in [0,1]} \tag{5.1}$$

$$\sum a_i^2 + b_i^2 = 1$$

*In order to show equivalence one must assume that P is an arcwise connected set and that $\{F(A,x) \mid \max |F(A,x)| \leq M\}$ is closed under pointwise convergence.

This is the classical example of a varisolvent function. Let

$$P_k = \{A \mid a^n = a^{n-1} = \ldots = a^{n-k} = b^m = b^{m-1} = \ldots = b^{m-k} = 0\} \tag{5.2}$$

If $A \in P_k$ and $A \notin P_{k+1}$ then the degree of A is

$$m(A) = n + m - k + 1 \tag{5.3}$$

Normally we have $k = 0$.

2. *Exponential functions* [7].

$$E(A,x) = \sum_{i=1}^{k} \left[\sum_{j=0}^{mi} a_{ij} x^j \right] e^{t_i x} \qquad |a_{ij}|, |t_i| < \infty \tag{5.4}$$

$$\sum_{i=1}^{k} (m_i + 1) \le n \tag{5.5}$$

This is the approximating function one obtains when the definition of the function $\sum_{i=1}^{n} a_i e^{t_i x}$ is extended to include the polynomial limits. The degree of A is

$$m(A) = n + \sum_{i=1}^{k} (m_i + 1) \tag{5.6}$$

3. *Constrained linear functions* [6].

$$L_c(A,x) = \sum_{i=1}^{n} a_i \varphi_i(x) \tag{5.7}$$

where the ith parameter a_i is constrained to lie in the open interval I_i. Condition (2.5) is assumed. Then the degree of A is

$$m(A) = n \tag{5.8}$$

4. *Exponential Cosine* (Conjectured).

$$E_c(A,x) = a e^{tx} \cos(\theta + \varphi x) + b \qquad \begin{matrix} |a|, |b|, |t| < \\ 0 \le \theta, \varphi \le \pi \end{matrix} \tag{5.9}$$

5. *Logarithmic* (Conjectured), $x \in [-1,1]$.

$$\text{(5.10)} \quad \text{Log}(A,x) = \sum_{i=1}^{n} a_i \log(1+b_i x) \qquad \begin{matrix} |a_i| < \infty \\ -1 < b_i < +1 \end{matrix}$$

6. *Exponential ratio* (Conjectured).

$$\text{(5.11)} \quad E_R(A,x) = \frac{\sum_{i=1}^{n} a_i e^{t_i x}}{\sum_{i=1}^{m} b_i e^{s_i x}} \qquad \begin{matrix} |a_i|, |b_i| < \infty \\ |t_i|, |s_i| < \infty \end{matrix}$$

6. COMPUTATION METHODS.

At the present time only a few computational methods are known to apply to these examples. See [4], [9] for some discussion of these methods. There is a conjecture however that the Remez algorithm [9] may be modified so as to apply to all varisolvent functions. The basis idea of this method is illustrated in Figure 9.

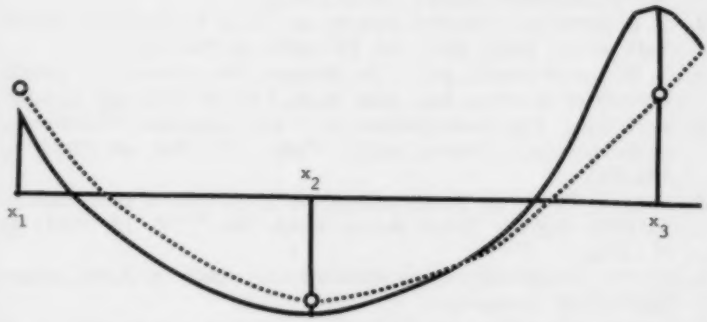

Figure 9. The Remez Algorithm for $m(A_k) = 3$.

One is given an estimate $F(A_k,x)$ of the best approximation to $f(x)$. It is required that the error curve $F(A_k,x) - f(x)$ alternates $m(A_k)$ times. If it does not one chooses the $m(A_k)$ largest local extrema of the error curve which have alternating signs. These occur at x_1, x_2 and x_3 in Figure 9. One then finds the estimate $F(A_{k+1},x)$ to the best approximation $F(A^*,x)$ which alternates *on these points* i.e., x_1,

x_2 and x_3. This approximation is shown in dotted line. It is known that this algorithm converges for linear approximating functions and some nonlinear ones [4], [8], [9]. It is conjectured that it converges for all varisolvent approximating functions.

There is one essential modification that must be made to this algorithm due to the varisolvence of the approximating functions. If $F(A_k,x)$ is of degree, say 5, it is possible that the degree of $F(A_{k+1},x)$ may be less, say 3. This implies that one cannot find any $F(A,x)$ that alternates 5 times on the six local extrema of $F(A_k,x) - f(x)$. This will, of course, become apparent during the process used to compute $F(A_{k+1},x)$. In such a case, one knows that the degree of $F(A_{k+1},x)$ is less than 5 and hence one replaces the 6 extrema by 5 extrema with largest size and with alternation. One then again attempts to compute $F(A_{k+1},x)$. One proceeds in reducing the number of extrema used until $F(A_{k+1},x)$ is found.

REFERENCES

1. N. I. Achieser, *Theory of Approximation*, Chapter II, New York, Ungar (1956).
2. Serge Bernstein, *Lecons sur les propriétés extremáles et la meillure approximation des fonctions analytiques d'une variable réelle*, Gauthier-Villars, Paris (1926).
3. T. S. Motzkin, *Approximation by curves of a unisolvent family*, Bull. Amer. Math. Soc., Vol. 55 (1949) pp. 789-793.
4. E. N. Novodworskii and I. Sh. Pinsker, *On a process of equalizations of maxima*, Usp. Mat. Nauk, Vol. 46 (1951) pp. 174-181.
5. J. R. Rice, *The characterization of best nonlinear Tchebycheff approximations*, Trans. Amer. Math. Soc., Vol. 96 (1960) pp. 322-340.
6. ———, *Tchebycheff approximation by functions unisolvent of variable degree*, Trans. Amer. Math. Soc., Vol. 99 (1961) pp. 298-302.
7. ———, *Chebyshev approximation by exponentials*, J. Soc. Indust. Appl. Math. to appear.
8. ———, *Algorithms for Chebyshev approximation by* $ab^x + c$. J. Soc. Indust. Appl. Math. to appear Dec. 1961.
9. E. L. Stiefel, *Numerical methods of Tchebycheff approximation*, in "On Numerical Approximation," edited by R. E. Langer, U. Wisc. Press (1959).
10. L. Tornheim, *On n-parameter families of functions and associated convex functions*, Trans. Amer. Math. Soc., Vol. 69 (1950) pp. 457-467.

INDUSTRIAL MATHEMATICS is published semi-annually by the Industrial Mathematics Society. The advance subscription price is $4.00 per annual volume of two issues. Back issues (one volume per year) are available at $3.00 per copy. Orders accompanied by check or money order should be addressed to Industrial Mathematics Society, 100 Farnsworth Street, Detroit 2, Michigan.

INDUSTRIAL MATHEMATICS contains original articles as well as expository articles dealing with the application of mathematics in industry. Persons having such manuscripts for publication should submit them in duplicate to the Editor, INDUSTRIAL MATHEMATICS, 100 Farnsworth Street, Detroit 2, Michigan. Any questions on editorial matters should be similarly addressed.

Manuscripts should be typed double-spaced on one side of $8\frac{1}{2}$ by 11 inch paper in complete and finished form precisely as they are to appear, and sent – packed flat – to the Editor. Where possible, Figures should be numbered consecutively in arabic numerals. Tables should be numbered in arabic numerals, and both figures and tables should have captions.

Authors will receive galley proofs for correction purposes. One-hundred reprints without covers will be furnished free.

Author's institutions or companies are asked to pay a publication charge of $7.50 per printed page for articles accepted for publication.